First evidences of PAMAM dendrimer internalization in microorganisms of environmental relevance: A linkage with toxicity and oxidative stress

Soledad Gonzalo, Ismael Rodea-Palomares, Francisco Leganés, Eloy García-Calvo, Roberto Rosal, Francisca Fernández-Piñas. First evidences of PAMAM dendrimer internalization in microorganisms of environmental relevance: A linkage with toxicity and oxidative stress. Nanotoxicology, 9, 706-718, 2015.

https://doi.org/doi: 10.3109/17435390.2014.969345

https://www.tandfonline.com/doi/abs/10.3109/17435390.2014.969345

First evidences of PAMAM dendrimer internalization in microorganisms of environmental relevance: A linkage with toxicity and oxidative stress

Soledad Gonzalo‡, Ismael Rodea-Palomares†, Francisco Leganés†, Eloy García-Calvo§, Roberto Rosal‡§, Francisca Fernández-Piñas†*

† Departamento de Biología, Facultad de Ciencias, Universidad Autónoma de Madrid, E-28049, Madrid, Spain

‡ Departamento de Ingeniería Química, Universidad de Alcalá, E-28871, Alcalá de Henares, Madrid, Spain

§ Advanced Study Institute of Madrid, IMDEA-Agua, Parque Científico Tecnológico, E-28805, Alcalá de Henares, Madrid, Spain

* Corresponding author: francisca.pina@uam.es

Abstract

This article reports novel results on the toxic mechanisms of action of amine- and hydroxyl-terminated poly(amidoamine) dendrimers towards microorganisms of environmental relevance, namely a cyanobacterium of the genus Anabaena and the green alga *Chlamydomonas reinhardtii*. We used PAMAM ethylenediamine core dendrimers from generations G2 to G4, which displayed a positive charge, measured as ζ-potential, in culture media. All amine-terminated and most remarkably the G4 hydroxyl-terminated dendrimer inhibited the growth of both microorganisms. The effect on the growth of the green alga was significantly higher than that on the cyanobacterium. With concentrations expressed in terms of molarity, there was a clear relationship between dendrimer generation and toxicity, with higher toxicity for higher generation. Hormesis was observed for hydroxyl-terminated dendrimers at low concentrations. The cationic dendrimers and G4-OH significantly increased the formation of reactive oxygen species (ROS) in both organisms. ROS formation was not related with the chloroplast or photosynthetic membranes and photosystem II photochemistry was unaffected. Cell damage resulted in cytoplasm disorganization and cell deformities and was associated to an increase in ROS formation and lipid peroxidation in mitochondria in the green alga; cell wall and membrane disruption with apparent loss of cytoplasmic contents was found in the cyanobacterium. It was determined for the first time that cationic PAMAM dendrimers were quickly and largely internalized by both organisms. These results warn against the generalization of the use of dendrimers which may pose significant risk for the environment and particularly for primary producers which are determinant for the health of natural ecosystems.

Keywords: Algae; PAMAM dendrimers; Cyanobacteria; Internalization; Mitochondrial damage.

1. Introduction

Poly(amidoamine) (PAMAM) dendrimers are hyper-branched polymeric, nanoscale molecules with exceptional properties that make them attractive for a variety of biomedical applications (Svenson and Tomalia, 2005). They consist of a central alkyldiamine core, from which radially branched monomers or dendrons grow in successive layers, called generations. Their nanostructure presents three main features from which their applications give raise. First, they are globular and highly symmetric as a result of which they possess an unusually low solution viscosity. Second, they have a large number of surface end-groups, which make them highly tunable in terms of solution chemistry. Finally, the presence of relatively large internal cavities allows remarkable core encapsulation ability (Caminade et al., 2005, Kim and Lamm, 2012).

Surface charge and molecular size have been found to determine cell permeability profiles and cytotoxicity. Cationic PAMAM dendrimers have been connected to a higher cytotoxic response due to their greater permeation rates in comparison with neutral or negatively charged dendrimers (Jain et al., 2010). It has also been shown that for the same kind of dendrimer, lower generations exhibit considerably less cytotoxicity than higher generation dendrimers (Menjoge et al., 2010). The modification of dendrimer surface groups has been shown to modulate the mechanism of cellular uptake of dendrimers and their conjugates across cell barriers (Saovapakhiran et al., 2009).

Dendrimers have proved their excellence as drug carriers with great potential in biomedical and pharmaceuticals applications because they can enhance the bioavailability of poorly water-soluble drugs and are able to provide effective interaction with cells. However, the evidence that dendrimers are largely internalized has raised questions regarding their potential cytotoxicity not only in humans but also in the environment as they may be eventually released and become a waste in different environmental compartments. The occurrence of

dendrimers in the environment has not yet been reported. Consequently, there are still no data available on their concentrations in environmental water bodies. It is interesting to note that current analytical techniques make it impossible the quantification of dendrimers in aqueous matrixes within the range of expected environmental concentrations, which in the case of most anthropogenic pollutants is in the ng/L to µg/L range (Uclés et al., 2013). Consequently, they are not likely to be detected unless they reach relatively high concentrations, which could be the case in view of their expanding range of applications. The toxicity of dendrimers has been mostly studied in a number of human cell lines (Jain et al., 2010). In general, the toxic effect has been found to increase with dendrimer generation and, in the case of dendrimers bearing positive charge, it has been attributed to a charge interaction with negatively charged biological membranes (Stasko et al., 2007). This interaction results in membrane disruption via nanohole formation (Leroueil et al., 2007). In most cases the toxicity of dendrimers has been linked to the generation of reactive oxygen species (ROS) (Mukherjee et al., 2010).

In spite of the relatively large amount of information available on the toxicity of dendrimers to human cell lines, their ecotoxicological characterization has received much less attention (Santiago-Morales et al., 2013, Ulaszewska et al., 2012). Most studies have focused on the effect of dendrimers on growth or cell viability of a few representatives of aquatic environments such as the marine bacterium *Aliivibrio fischeri* (Mortimer et al., 2008, Naha et al., 2009), green algae such as *Chlamydomonas reinhardtii* and *Pseudokirchneriella subcapitata* (Perreault et al., 2012, Petit et al., 2012, Petit et al., 2010, Suarez et al., 2011), *Daphnia magna* (Naha et al., 2009) and zebrafish embryos (Heiden et al., 2007). However, very few mechanistic studies have been done (Petit et al., 2012) and no internalization data are available.

In this paper, the effects of amine- and hydroxyl-terminated PAMAM dendrimers were investigated using microorganisms of environmental relevance, namely two primary freshwater producers, a green alga and a cyanobacterium. The aim was to get an insight into dendrimer toxicity for an exposure scenario associated to the discharge of dendrimers into the aquatic environment. We determined toxicity endpoints and performed mechanistic studies by measuring ROS formation, membrane lipid peroxidation, cell ultrastructure changes and photosynthesis. The internalization of dendrimers was also tracked for cationic dendrimers using conjugates with the fluorescent label Alexa Fluor.

2. Methods

2.1 Characterization of dendrimers

Amine- and hydroxyl terminated G2, G3 and G4 PAMAM ethylenediamine core dendrimers, where G stands for generation, were provided by Sigma-Aldrich (St. Louis, MO, USA) or directly from the vendor Dendritech Inc. (Midland, MI, USA). Sigma-Aldrich supplies dendrimers 10-20% in methanol while Dendritech provided methanol-free aqueous solutions. Comparison of methanol containing samples and methanol free ones did not produce any significant difference in the organism response (data not shown), therefore, dendrimer stock suspensions were used interchangeably. The size distribution of nanoparticles was obtained using dynamic light scattering (DLS, Malvern Zetasizer Nano ZS). The measurements were conducted at the lowest possible concentration yielding reproducible results. ζ-potential was measured via electrophoretic light scattering combined with phase analysis light scattering in the same instrument, the measurements being conducted at 25ºC in the assay media without any modification.

2.2 Physicochemical characterization of cells

Cell size was estimated from a representative number of TEM images; ζ-Potential of cells of both organisms was measured in three independent cell culture suspensions in their respective exposure media (AA/8+N for Anabaena sp. PCC7120, and Sueoka's high salt medium for *C. reindhartii*, see below). Measurements were performed at the pH of the bioassays (pH = 7.4). ζ- Potential measurements of cell suspensions were conducted essentially as described above, using electrophoretic light scattering combined with phase analysis in a Malvern Zetasizer Nano ZS.

For Fourier Transform Infrared (FTIR) analyses, algal cells were grown as described, centrifuged, and washed with Na salts as described (Dittrich and Sibler, 2005, Hadjoudja et al., 2010, Kiefer et al., 1997); briefly two times with 0.2 M NaCl, and finally resuspended in 0.2 M NaCl to a final cell density of 20-50 mg algae/mL. Algal suspensions were dropped in KBr discs and dried on them at room temperature during 2h. Finally, KBr discs containing the dried algal material were measured using a Bruker model IFs 66V Fourier Transform Infrared (FTIR) spectrometer in transmission mode; the spectra were recorded with 250 scans and a resolution of 4 cm^{-1} with spectral range of 7,000 to 550 cm^{-1}.

2.3. Growth and photosynthesis assessment of algae and cyanobacteria

The filamentous cyanobacterium Anabaena sp. PCC 7120 was routinely grown as described (Rodea-Palomares et al., 2012). The green alga *Chlamydomonas reinhardtii* was grown at 28ºC in the light, Ca. 65 µmol photons m^2 s^{-1} with soft aeration with sterile synthetic air in 250 ml in Sueoka's high salt medium (HS) (Sueoka, 1960). For both microorganisms, exposure experiments were carried out in 12 mL of AA/8, which is an 8-fold dilution of the medium of Allen and Arnon (1955), for the cyanobacterium and HS for the green algae in 25 mL Erlenmeyer flasks. The pH of both culture media was adjusted to 7.4. Before exposure to dendrimers, cultures were washed once and resuspended in their proper culture media to obtain a final optical density (DO 750

nm) of 0.1. PAMAM dendrimers were added to obtain the desired concentrations and cultures were exposed for up to 72 h in a rotary shaker at 28ºC under constant illumination. Growth inhibition experiments were performed essentially as previously described (Rodea-Palomares et al., 2011). In-vivo fluorescence of chlorophyll was measured daily by transferring 100 μL of quadruplicate samples of cultures to an opaque black 96 well microtitter plate and by measuring with 485/645 excitation/emission wavelengths on a Synergy HT multi-mode microplate reader (BioTek,USA). Chlorophyll determinations for the cyanobacterium were made according to the method of Marker (Marker, 1972). For total chlorophyll determinations (chlorophyll a + b) of *Chlamydomonas reinhardtii*, according to the method of Porra (Porra et al., 1989). The maximum photosynthetic efficiency of photosystem II (PS II) expressed as the dark adapted Fv/Fm ratio parameter was calculated from chlorophyll a fluorescence emission measurements using amplitude modulated (PAM) fluorometry (Hansatech FMS fluorometer, Hansatech, Inc, UK) essentially as previously reported (Rodea-Palomares et al., 2012).

2.4. Detection of reactive oxygen species (ROS)

Control and treated cells were loaded with the fluorescent dyes 2',7'-dichlorofluorescein diacetate (H2DCFDA) whose intracellular oxidation originates 2,7-dichlorofluorescein (DCF) and C4-BODIPY® (Invitrogen Molecular Probes; Eugene, OR, USA) (Gomes et al., 2005). Mitochondrion-selective probes (MitoTracker Green FM and MitoTracker Orange CM-H2 TM ROS (Invitrogen Molecular Probes; Eugene, OR, USA) were used to target mitochondria and evaluate possible alterations of mitochondrial ROS homeostasis.1 mM MitoTracker Green FM and MitoTracker Orange CM-H2 TM ROS was freshly prepared in DMSO under dim light conditions to avoid degradation. C. reinhardtii cells were incubated for 1h with 200 nM and 500 nM (final concentration) of MitoTracker Green FM and MitoTracker Orange CM-H2 TM ROS, respectively. For the determination of intracellular ROS level, the procedure as detailed in Rodea-Palomares et al. (2012) was followed. Fluorescence was monitored on a Synergy HT multi-mode microplate reader (BioTek, USA) with excitation and emission wavelengths of 488 and 530 nm, respectively.

2.5. Internalization studies

The Alexa Flour 488 reactive dye has a tetrafluorophenyl (TFP) ester which reacts efficiently with primary amines to form stable fluorescent dye-protein conjugates with excitation and emission maxima of 494 nm / 519 nm. PAMAM-Alexa Fluor 488 conjugates were prepared essentially following the standard protocol of the Alexa Fluor 488 microscale protein labelling kit (A30006, Molecular probes). Briefly, 10 μL of reactive dye was added to 1mg/mL of G2, G3 and G4 PAMAM dendrimer solutions prepared in MiliQ water and was subsequently prepared following the commercial protocol. This amount of reactive dye was calculated based on a molar ratio of 5. Due to the symmetry of the increase in molecular weight and surface primary amino groups (1, 2, 4, increasing factor for G2, G3 and G4, respectively), a fixed amount of dye allowed marking a constant number of functional groups per molecule. The experimental degree of labeling (DOL), the final concentration of marked dendrimers, and the experimental number of functional groups per mL, were calculated essentially as proposed by the producer's protocol (see Supplementary Table S1). Due to the closeness of the results and easiness in subsequent experimental procedures, all PAMAM-Alexa Fluor 488 conjugates (G2, G3 and G4) were considered to have a nominal PAMAM concentration of 500 mg/L and a homogeneous DOL. At the end of the internalization experiments, data were corrected according to the real experimental concentrations and DOL of each dendrimer. In order to discriminate surface bound and truly internalized dendrimers, Anti-Alexa fluor 488 Rabbit IgG Fraction (A-11094, Molecular probes), was used. This antibody specifically links with Alexa488 dye producing a highly efficient quenching of the fluorescence signal. The recommended amount of Anti-Alexa fluor 488 antibody [2μl of antibody solution (1mg/mL) for quenching 1mL of 5 nM Alexa Fluor 488 solution] together with 1/10 and 1/100 dilutions were evaluated for their quenching potency of the fluorescence of the PAMAM-Alexa Fluor 488 conjugates in incubation times of 10 min and 60 min by flow cytometry. We did not find statistically significant differences in the quenching of fluorescence emission for incubation times in the 10-60 min range or between recommended and 1/10 and 1/100 dilutions. A final exposure time of 10 min and a 1/100 dilution of Anti-Alexa488 antibody were used. Internalization calculations were made as explained in Table S1.

2.6 Microscopy

DCF, chlorophyll a, PAMAM-Alexa fluor 488 conjugates and C4-BODIPY® fluorescence in cells were visualized using a confocal fluorescence microscope (Espectral Leica TCS SP5) with excitation at 488 nm. The emission filter was settled at 665 nm for chlorophyll fluorescence visualization and 535 nm for fluorescence markers (DCF, C4-BODIPY® and PAMAM-Alexa fluor 488 conjugates). Images were acquired with a Leica Confocal Software (LCS Lite) and processed using Adobe Photoshop 9.0 (Adobe Systems Inc., USA). All comparative images (treated vs. untreated samples) were obtained under identical microscope and camera settings. For transmission electron microscopy, the procedure described in Rodea-Palomares et al. (2011) was followed.

2.7. Flow cytometry

Chlorophyll (cell autofluorescence), DCF fluorescence, lipid peroxidation (C4-BODIPY®) and internalization of PAMAM-Alexa fluor 488 conjugates were evaluated using a Cytomix FL500 MPL flow cytometer (Beckman Coulter Inc., Fullerton, CA, USA). Setting adjustments of the equipment, data acquisition and analysis and measurements of chlorophyll, DCF and C4-BODIPY®

fluorescence were performed as detailed elsewhere (Rodea-Palomares et al., 2012).

2.8. Data analysis

All tests of statistically significant differences between datasets were performed with the appropriate post hoc test depending on the characteristics of datasets. For single comparison of two means, Student's t-tests at $p < 0.05$ was used, when multiple comparison of means were performed, ANOVA test was used with at $p < 0.05$ as significant criteria with R software. In flow cytometry analyses, statistically significant differences were assessed by the Kolmogorov-Smirnov test ($P < 0.05$) due to non-normality of frequency distributions of the histograms, using CXP-2.2 software. Effective concentration values (EC_x) were computed by using dose-response curve (drc) package version 2.2-1 for R software. Best fit dose-response model was chosen based on the best log likelihood value and the minimization of the residual of variances. Once the best fit model was selected, EC_x values and their 95% confidence intervals were computed based on the asymptotic-based confidence intervals.

3. Results

3.1 Physicochemical characterization of PAMAM dendrimers and cells

The properties of the amine- and hydroxyl terminated G2, G3 and G4 PAMAM ethylenediamine core dendrimers in pure water and in culture media are shown in Table 1. Data correspond to water and culture media without cells. The hydrodynamic diameter of dendrimers as measured by dynamic light scattering (DLS) revealed the presence of aggregates of a few hundreds of nanometers. In pure unbuffered water at pH 6.5 we could observe peaks in the 2-5 nanometer range representing a low percentage of the intensity signal, but dominant in the number distributions determined from Mie's theory. These signals correspond to the size of individual molecules in the PAMAM series, which increased from 2.9 to 4.5 nm for the G2-G3-G4 series according to the producer (PAMAM-NH_2 series) and appear together with a single peak corresponding to aggregates. Due to the nature of the simplifications assumed for converting intensity into number or volume distributions in multimodal samples, these data cannot be considered absolute. However, they indicate the presence of a large number of individual dendrimers in solutions, which coexist with aggregates two orders of magnitude larger. For the lower concentrations, for example when passing from 20 μM to 2.0 μM in the case of G2-OH, the intensity signal for individual dendrimers would become not detectable, the suspension appearing as perfectly monodisperse. DLS is not a particularly sensitive technique for PAMAM dendrimers because of their refractive index, which is similar to that of the water (Chu, 2008). For this reason, the intensity of scattering is low, making it difficult to obtain a consistent size measurement for low concentrations. Those indicated in Table 1 are the lowest concentrations for which we could obtain consistent and reproducible results. For dendrimers in AA/8 and HS media, the suspensions appeared as perfectly monodisperse, with aggregates in the hundreds of nanometer range, slightly higher than those measured in the same media without dendrimers. This probably indicates the adsorption of dendrimers on the surface of the pre-existing particles of salty media.

Table 1. Particle hydrodynamic size determined by dynamic light scattering, and ζ-potential measured by electrophoretic light scattering with their95% confidence intervals. The data correspond to ζ-potential and size of aggregates in water and culture media without cells.

Size (nm)	Pure Water pH 6.5	AA/8 (*) pH 7.4	HS (*) pH 7.4
without dendrimer	-	354 ± 90	217 ± 14
G2-OH	2.94 ± 0.23 (1) 227 ± 18 (2)	371 ± 59 (1)	325 ± 27 (1)
G3-OH	3.52 ± 0.40 (3) 214 ± 24 (4)	340 ± 36 (3)	331 ± 34 (3)
G4-OH	4.27 ± 0.33 (5) 205 ± 12 (6)	482 ± 60 (5)	269 ± 21 (5)
G2-NH2	2.25 ± 0.44 (1) 212 ± 37 (2)	437 ± 39 (1)	306 ± 25 (1)
G3-NH2	4.27 ± 0.20 (3) 205± 18 (4)	385 ± 43 (3)	266 ± 11 (3)
G4-NH2	4.78 ± 0.49 (5) 190 ± 8 (6)	356 ± 30 (5)	344 ± 15 (5)
ζ-potential (mV)	Pure Water pH 6.5	AA/8 (*) pH 7.4	HS (*) pH 7.4
without dendrimer	-	-22.6 ± 0.7	-4.80 ± 1.80
G2-OH	+8.99 ± 0.75 (1)	+16.2 ± 1.1 (1)	+12.3 ± 0.7 (1)
G3-OH	+9.42 ± 1.10 (3)	+17.0 ± 1.2 (3)	+14.8 ± 3.3 (3)
G4-OH	+10.8 ± 0.6 (5)	+20.3 ± 0.2 (5)	+11.5 ± 3.6 (5)
G2-NH2	+7.18 ± 0.58 (1)	+12.3 ± 0.7 (1)	+15.2 ± 2.4 (1)
G3-NH2	+20.6 ± 1.9 (3)	+22.3 ± 2.5 (3)	+20.3 ± 4.2 (3)
G4-NH2	+27.2 ± 1.5 (5)	+35.1 ± 2.2 (5)	+34.8 ± 4.6 (5)

(1) 20 μM, (2) 2.0 μM, (3) 10 μM, (4) 1.0 μM, (5) 5 μM, (6) 2.5 μM,
(*) AA/8 is a 8-fold dilution of the medium of Allen and Arnon (1955) and HS stands for Sueoka's high salt medium (1960). They were used to culture cyanobacteria and algae respectively.

The charge of all dendrimers was positive in pure water at pH6.5 and in the growth media of cyanobacteria and algae at the bioassay pH (7.4). This net positive charge can be attributed to the secondary and tertiary amines forming the dendrimer structure. The concentration indicated for ζ-potential measurements in Table 1 was again the lowest for which we could obtain reproducible data, the signal-to-noise ratio being too low to get reliable electrophoretic determinations for lower concentrations. In the culture media used for cyanobacteria (AA/8) and algae (HS), we could observe negatively charged nanoparticles with sizes in the 200-400 nm range, the size of which increased in the presence

Table 2. Physicochemical characterization of *Chlamydomonas reinhardtii* and *Anabaena* sp. PCC7120 cells in exposure media

Chlamydomonas reinhardtii			
Cell size (as estimated by TEM)	Surface charge (ζ-potential; pH: 7.4)	Wavenumber (cm^{-1})	Peak assignment
8-10 µm	-15.30 ± 1.08	3500	Amide A
		3200	Amide B
		2923	C-H sp^3 asymmetric stretching vibrations
		2852	C-H sp^3 symmetric stretching vibrations
		1618	Amide I Band (C=O stretching vibrations in proteins)
		1460	to $-CH_2$ and $-CH_3$ stretching vibrations in proteins
		1384	stretching vibrations of CH_2 and CH_3 and/or vending vibrations from C-O bond in carboxylic acids
		1320	C-O stretching vibration in carboxylic acids
		1200-800	vending vibration of C-O-C and C-O bonds in polysaccharides
Anabaena sp. PCC7120			
Cell size (TEM)	Surface charge	Wavenumber (cm^{-1})	Peak assignment
2-3 µm individual cells within filaments	-15.43 ± 2.2	3500	Amide A
		3200	Amide B
		2923	C-H sp^3 asymmetric stretching vibrations
		2852	C-H sp^3 symmetric stretching vibrations
		1618	Amide I Band (C=O stretching vibrations in proteins)
		1460	to $-CH_2$ and $-CH_3$ stretching vibrations in proteins
		1384	stretching vibrations of CH_2 and CH_3 and/or vending vibrations from C-O bond in carboxylic acids
		1320	C-O stretching vibration in carboxylic acids
		1200-800	vending vibration of C-O-C and C-O bonds in polysaccharides

of dendrimers. This is most probably because of the attachment of positively charged dendrimers to the negative surface of the particles in the media.ζ-potential increased in this case up to values close to those obtained in pure water, the results having been obtained with much better photon count intensities.

Relevant physicochemical properties of algal cells were also studied (Table 2). As estimated by a representative number of TEM images, the size of the algal cells varied between 8 and 10 µm while the individual cyanobacterial cell size ranged between 2-3 µm. The cell surface charge at the pH of the bioassays was negative as expected (Dittrich and Sibler, 2005, Hadjoudja et al., 2010) and quite similar for both organisms which share similar surface functional groups as obtained by FTIR (Table 2 and Fig.S1). FTIR spectroscopy is a sensitive tool for the study of microbial cell surface (van der Mei et al., 1989). FTIR analyses of both *C. Reindhartii* and Anabaena sp. PCC 7120 revealed absorption spectra in the infrared regions between 3700 cm-1 and 600 cm-1 clearly dominated by amide-type resonance and highly similar if not almost identical for both organisms. Both IR absorption spectra showed a strong absorption patter with multiple peaks found around 3500 cm^{-1} and 3200 cm^{-1} and 1618 cm^{-1}. Absorption peaks cantered at 3500 cm^{-1} and 3200 cm^{-1} may correspond to the amide A (about

3500 cm^{-1}) and amide B (about 3100 cm^{-1}) bands, respectively (resulting mainly from N-H stretching vibrations). The peak at 1616 cm^{-1} may be assigned to the Amide I band (between 1600 and 1700 cm^{-1}), mainly associated with the C=O stretching vibrations in proteins (Dittrich and Sibler, 2005, Kiefer et al., 1997). These peaks may then be assigned to functional groups present mainly in proteins which represent a significant part of the cell wall and membranes of both organisms: *C. reinhardtii* has a high proportion of hydroxyproline-rich glycoproteins in its cell wall (Goodenough and Heuser, 1985, Kiefer et al., 1997) and the cyanobacterium Anabaena sp. PCC7120 is a Gram negative bacterium with a characteristic peptidoglycan layer. In the spectra, it can also be observed a double peak of IR absorption at 2923 cm^{-1} and 2852 cm^{-1} corresponding to C-H sp^3 asymmetric and symmetric stretching vibrations of hydrocarbon backbones mainly from alkyl functional groups. Looking at the fingerprint region (from 1800 to 800 cm^{-1}), some small but specific absorption peaks can also be identified: a weak absorption peak at 1460 cm^{-1} has been previously assigned to -CH_2 and -CH_3 stretching vibrations in proteins, the well-defined peak at 1384 cm^{-1} has been assigned to stretching vibrations of CH_2 and CH_3 and/or vending vibrations from C-O bond in carboxylic acids. The peak at near 1320 cm^{-1} can be assigned to C-O stretching vibration in carboxylic acids (Dittrich and Sibler, 2005). Finally, the broad absorption band between 1200 cm^{-1} and 800 cm^{-1} has been typically assigned to the overall contribution of vending vibration of C-O-C and C-O bonds in polysaccharides (Dittrich and Sibler, 2005). This last broad region (1200 cm^{-1} and 800 cm^{-1}) is where the IR spectra of both organisms showed the most remarkable difference: In *C. reinhardtii*, its spectrum presents a higher absorption all throughout the region in comparison to Anabaena sp. PCC7120 spectrum (Fig. S1B and D). These differences may be explained by a higher contribution of polysaccharides to the total composition of the cell wall of *C. reindhartii* as compared to the cell wall of Anabaena sp. PCC7120, which has a thin layer of peptidoglycan with no exopolymeric substance (EPS) external layer (which implies a lower amount of polysaccharides) (Rodea-Palomares et al., 2011, Leganes et al., 2005).

3.2. Effect on the growth of cyanobacteria and algae

Table 3 shows the effects of hydroxyl-terminated and amine-terminated G2, G3 and G4 dendrimers on growth of the green alga *Chlamydomonas reinhardtii* and the cyanobacterium Anabaena sp. PCC 7120, dose-response profiles of the different PAMAM dendrimers for both *C.*

Table 3. Dose-effect parameters of toxicity (as growth inhibition) induced by PAMAM dendrimers for both *Chlamydomonas reinhardtii* and *Anabaena* sp. PCC7120 after 72h of exposure.

Chlamydomonas reinhardtii						
Compound	Model fitted[1]	Max. Stimulation[2]	Max. Inhibition[3]	EC_{10} (mg/L)	EC_{50} (mg/l)	EC_{90} (mg/l)
G2-OH	-	-	10 (30%)	-	-	-
G3-OH	-	-	10 (50%)	-	-	-
G4-OH	BC.5	0.27 (150%)	-	0.44^{a}(0.41-0.47)	0.74^{a}(0.69-0.78)	1.02^{a}(0.91-1.13)
G2-NH2	LL2.3u	-	-	0.50^{b}(0.49-0.52)	0.58^{b}(0.57-0.59)	0.71^{b}(0.69-0.74)
G3-NH2	W2.4	-	-	0.44^{a}(0.41-0.46)	0.56^{c}(0.48-0.64)	0.65^{b}(0.52-0.77)
G4-NH2	W1.4	-	-	0.55^{c}(0.53-0.56)	0.68^{a}(0.67-0.69)	0.78^{c} (0.75-0.81)
Anabaena sp. PCC7120						
Compound	Model fitted	Max. Stimulation	Max. Inhibition	EC_{10} (mg/l)	EC_{50} (mg/l)	EC_{90} (mg/l)
G2-OH	-	10 (105%)	0%	-	-	-
G3-OH	-	10 (105%)	0%	-	-	-
G4-OH	W1.3	-	-	2.66^{a}(1.80-3.52)	3.97^{a}(3.53-4.41)	5.13^{a}(4.49-5.77)
G2-NH2	LN.2	-	-	1.07^{b}(0.72-1.41)	1.76^{b}(1.49-2.03)	2.91^{b}(2.06-3.76)
G3-NH2	LL.3u	-	-	2.16^{a}(1.87-2.46)	2.57^{c}(2.43-2.71)	2.92^{b}(2.63-3.22)
G4-NH2	BC.5	-	-	2.56^{a}(2.32-2.78)	3.37^{d}(2.96-3.52)	4.53^{a}(3.77-5.12)

Statistically significant differences (ANOVA, *post hoc*, $p < 0.05$) for the different effective concentrations (EC_x) are indicated by superscript letters.

[1]: Model fitted: Fitted models were selected based on the best fit offered by drc package for R. Notation for the selected fitted models is according to drc notation:BC.5. Brain Cousens model, LL2.3u: Log-logistic 2.3 U shaped, W2.4: Weibull model 2.4, W1.4: Weibull model 1.4, W1.3: Weibull model 1.3, LN.2: Log-normal 2 parameters model, LL.3u: Log-logistic three parameters,

[2]: Max. Stimulation: Concentration at which the maximum stimulation occurred together with the % of stimulation (between parentheses) of the studied end-point respect to the control level.

[3]: Max.Inhibition: Concentration at which the maximum inhibition occurred together with the % of inhibition (between parentheses) achieved at that concentration.

reindhartii and Anabaena sp. PCC7120 from which information in Table 3 was derived can be found in supplementary material Fig. S2. The maximum growth inhibition for G2-OH in the green alga was 30% at the highest concentration tested (10 mg/L). A growth inhibition of 50% for that same concentration was found for G3-OH, both hydroxyl-terminated dendrimers being nontoxic for the cyanobacterium. In fact a mild hormetic response was recorded as growth was stimulated by 5% after treatment with both dendrimers at the highest concentration tested (10 mg/L). G4-OH was toxic for both organisms and, according to EC_{50} values, it was significantly (one order of magnitude) more toxic to the green alga than to the cyanobacterium. Noteworthy, a true hormetic effect (50% growth stimulation) was observed at very low concentrations in the green alga. In contrast to hydroxyl-terminated dendrimers, all the amine-terminated ones were toxic for both the green alga and the cyanobacterium. The cationic dendrimers were significantly more toxic to the green alga. The data in Table 3 are given in mass concentration units (mg/L). However, toxicity should also be analyzed considering the large differences in molecular weight of the tested dendrimers. To this end Supporting Information is given in Table S2 with dendrimer concentrations expressed in µM. It is clear that when concentrations are expressed in terms of molarity, there is a clear relationship between dendrimer generation and toxicity: the higher the generation, the higher the toxicity so that both G4 dendrimers showed the lowest (and quite similar) EC_x values indicating that they are the most toxic ones towards both organisms.

3.3. Oxidative stress and cell damage

Increasing evidence indicates that nanoparticles in general can generate reactive oxygen species (ROS) and subsequently oxidative stress ("the oxidative stress paradigm") which might eventually lead to cell damage and cell death (Xia et al., 2006). In order to investigate whether the tested hydroxyl-terminated and amine-terminated dendrimers elicited oxidative stress in *C. reinhardtii* and Anabaena, ROS formation was evaluated by fluorometry, flow cytometry and confocal microscopy using the fluorescence indicators DCF (general oxidative stress indicator) and C4-BODIPY (membrane lipid peroxidation).

Fig. 1shows the DCF fluorescence intensities normalized to the concentration of chlorophyll in the sample (as recorded by fluorescence spectrophotometry) and flow cytometry histograms representing DCF green fluorescence intensities (arbitrary units) versus number of cellular events (frequency) of *C. reinhardtii* (Fig. 1A) and Anabaena (Fig. 1B). In the green alga (Fig. 1A), the hydroxyl-terminated G2-OH and G3-OH significantly increased DCF fluorescence intensity at concentrations above 1 mg/L particularly after 48 hours of exposure. Fluorescence intensity returned to control levels after 72 h of exposure. This increase in ROS formation could be correlated to the mild growth inhibition observed at the higher concentration tested (Table 3). On the contrary, in the cyanobacterium (Fig. 1B), the hydroxyl-terminated G2-OH and G3-OH, which did not show any toxicity did not increase DCF fluorescence intensity at any of the tested concentrations. In the green alga (Fig. 1A), the toxic hydroxyl-terminated G4-OH PAMAM dendrimer increased DCF fluorescence intensity at concentrations above 0.4 mg/L after 48 h of exposure, indicating mild but significant ROS formation and highly increased DCF fluorescence after 72 h of exposure at concentrations above 0.75 mg/L. In the cyanobacterium (Fig. 1B), the toxic hydroxyl-terminated G4-OH PAMAM dendrimer mildly although significantly increased DCF fluorescence intensity at concentrations in the range between 1 and 4 mg/L after 24 h of exposure further inducing a high increase at concentrations above 4 mg/L which lasted throughout the experiment indicating significant ROS formation.

The three cationic dendrimers significantly increased DCF fluorescence in the green alga (Fig. 1A) after 48 h and, to a greater extent, after 72 h of exposure at concentrations above 0.1 mg/L indicating significant ROS formation which correlated with the observed high toxicity of these three dendrimers (Table 3). This is further confirmed by the flow cytometry histograms, which showed shifts to the right at these concentrations indicating subpopulations of cells with increased DCF fluorescence intensities and, therefore, increased ROS formation. In the case of the cyanobacterium (Fig. 1B), the three cationic dendrimers also significantly increased DCF fluorescence indicating ROS formation at concentrations above 1 mg/L and for shorter exposure times (24 h).The intensity of DCF fluorescence decreased for longer exposures. Flow cytometry histograms showed shifts to the right that were clearly significant after 24 h of exposure indicating subpopulations of cells with increased ROS formation. The observed decrease of DCF fluorescence for higher exposure is also reflected in shifts to the left in the flow cytometry histograms indicating filament fragmentation and eventually cell damage and death (Fig. S3). In addition, DCF fluorescence data showed that ROS formation, which may lead to oxidative stress, occurred at lower dendrimer concentrations in the green alga as compared to the cyanobacterium which agrees with a higher toxicity of dendrimers to the green alga (Table 3).

Fig. 2 shows confocal micrographs of DCF green fluorescence and chlorophyll red autofluorescence of both the green alga (Fig. 2A) and the cyanobacterium (Fig. 2B) exposed to 1.5 mg/L of G2-NH2 (as representative of toxic cationic PAMAM dendrimers) for 24 h. Optical micrographs of the green alga (Fig. 2A) show cell protrusions or deformities, which are more pronounced in the underneath cell. Chlorophyll autofluorescence indicated that both cells shown in Fig. 2Awere viable. Interestingly, DCF fluorescence (ROS formation) in the cells was not uniform and there was a clear area of the cell that in the overlay image seemed to

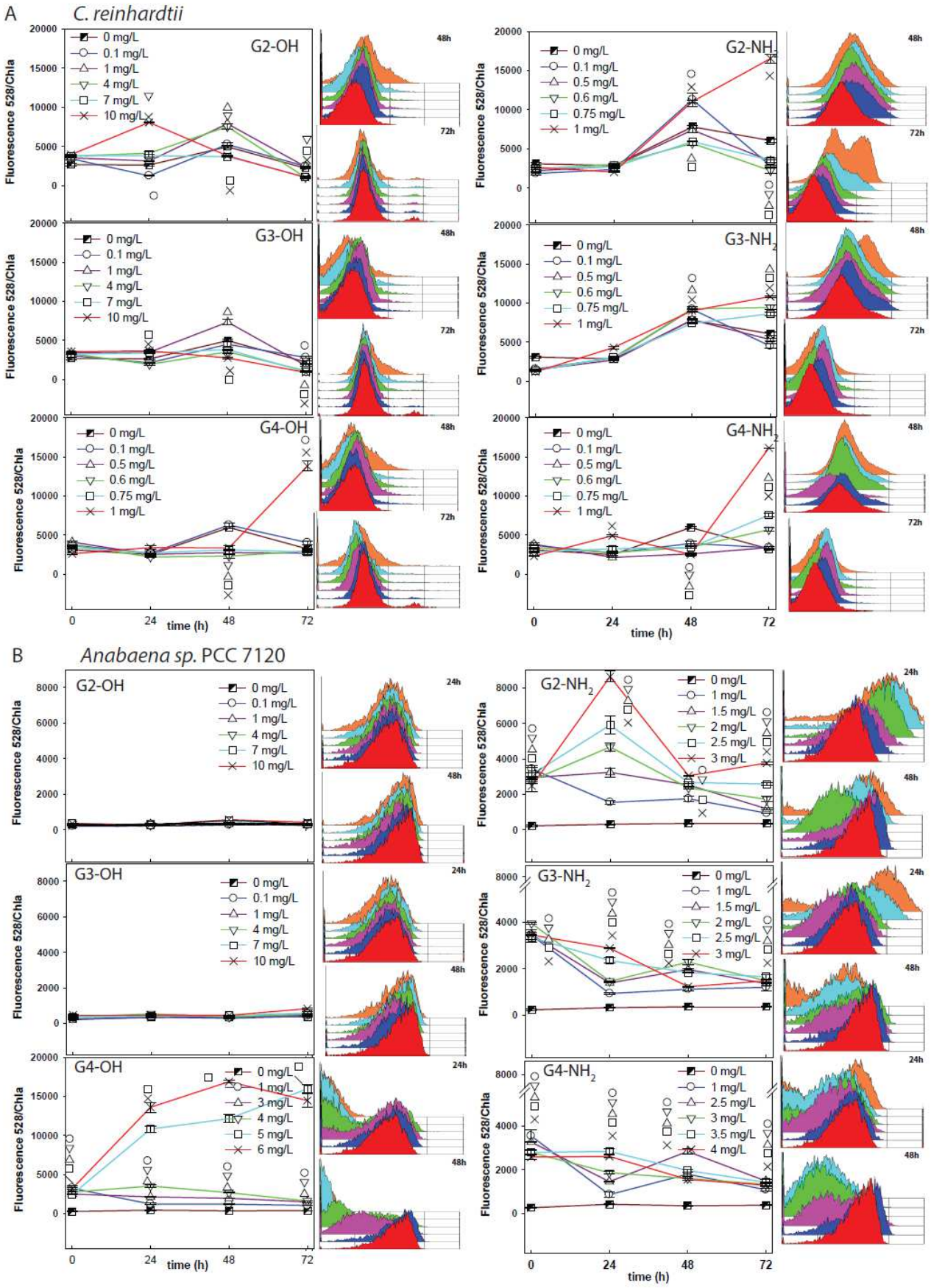

Figure 1. Oxidative stress in *C. reinhardtii* (A) and *Anabaena* PCC7120 (B) cells exposed during 72h to $-NH_2$ and –OH surface terminated PAMAM dendrimers. Oxidative stress was measured by recording the fluorescence emission of DCF (480/528nm), by microplate fluorometry (expressed as Fluorescence/Chl *vs* time) and flow cytometry, presented as frequency histograms (frequency vs FL1 intensity). Statistically significant differences with control untreated cells (ANOVA, post hoc, $p<0.05$) are indicated with the correspondent symbol in the figure.

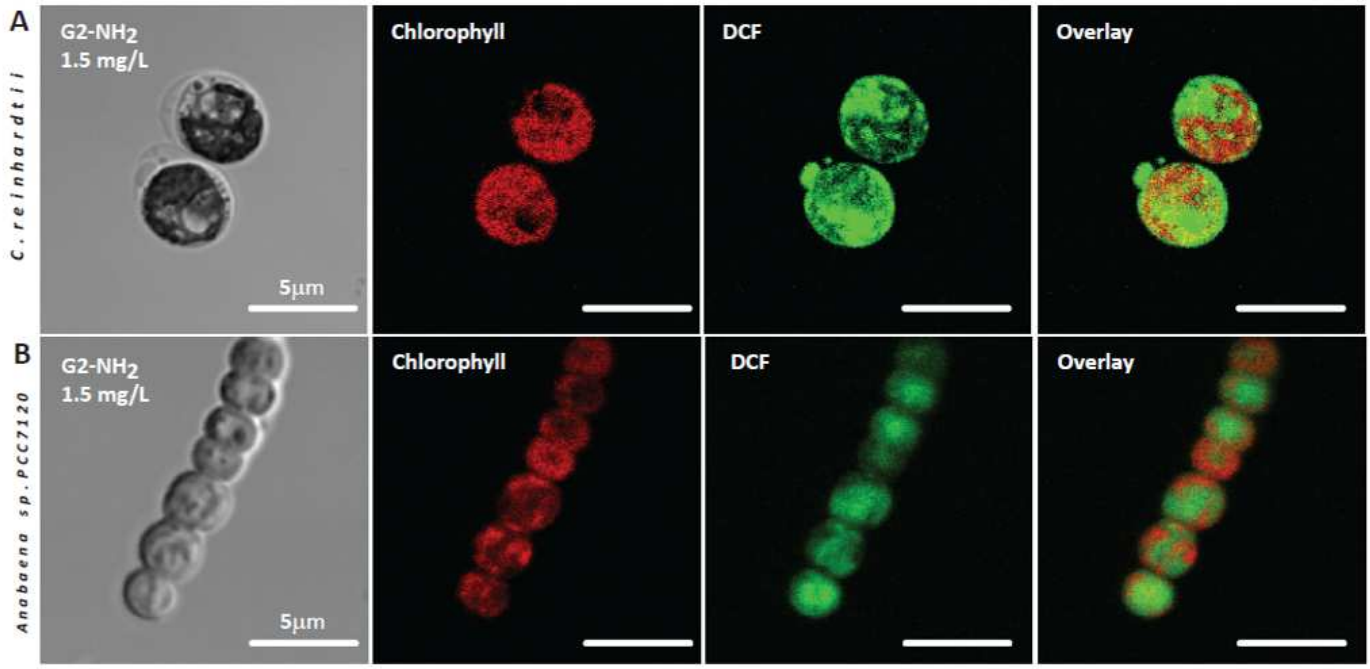

Figure 2. Cellular localization of ROS signal induced by $–NH_2$ PAMAM dendrimers. Representative confocal images of (A) *C. reinhardtii* and (B) *Anabaena* PCC7120 cells exposed to 1.5 mg/L of G2-NH_2 PAMAM dendrimers. Images are (left to right) bright field, chlorophyll fluorescence (red), DCF fluorescence (green) and overlay.

correspond to the chloroplast that showed less or no green fluorescence. This suggested that ROS formation was not related with photosynthetic membranes. In the underneath cell there was a clear DCF fluorescence signal in the cytoplasmic deformity. A representative filament of the cyanobacterium is shown in Fig. 2B. High DCF fluorescence was clearly visible in every cell of the filament. However, as in the case of the green alga, the fluorescence was not uniformly distributed within the cell and, as shown in the overlay image, the cell areas with less or no DCF fluorescence were the thylakoids (photosynthetic membranes). These results suggest that ROS formation did not occur in photosynthetic membranes either in the alga or in the cyanobacterium.

Nevertheless, as photosynthesis is one of the main cellular targets of oxidative damage, we checked whether the photosynthetic machinery of both organisms was affected by dendrimers by measuring chlorophyll a fluorescence emission. This technique is a non-destructive measure used to detect and estimate the status of photosystem II (PSII), which is the main site that is highly susceptible to many environmental stresses in photosynthetic organisms (Geoffroy et al., 2007). Fig. S4 shows the dark adapted Fv/Fm ratio of the cyanobacterium and alga in the presence of increasing concentrations of dendrimers; this parameter is used as an indicator of maximum photosynthetic performance; it reflects the potential maximum of PSII quantum yield or quantum efficiency of open PSII centres (Maxwell and Johnson, 2000). As observed in the figure, there were not relevant differences with any of the treatments in a dose-effect manner as compared to the control indicating that photosynthesis was not targeted by dendrimers. TEM micrographs (Fig. 3B, C) confirm the presence of cytoplasmic deformities in dendrimer-exposed green algal cells possibly owing to chloroplast shrinkage and subsequent cell disorganization. The observed protrusion may indicate plasma membrane disruption. Anyway, there was no loss of cytoplasmic contents because, as observed, the cell wall, made primarily of hydroxyproline-rich glycoproteins, was apparently well preserved. Mitochondria were clustered (condensed) within protrusions, some of them swollen with loss of cristae. We also observed electron dense granules, probably small vacuoles.TEM micrographs of Anabaena (Fig. 3F, G) cells showed cell wall and membrane disruption with apparent loss of cytoplasmic contents. Lipid peroxidation was revealed by the C4-BODIPY fluorescent dye. Flow cytometry histograms indicate lipid peroxidation in *C. reinhardtii* (Fig. 4A) but not in Anabaena PCC7120 (Fig. 4B) cells exposed to 1.5 mg/L G2-NH2 PAMAM dendrimers. Confocal images showed that BODIPY green fluorescence in the green alga (Fig. 4C) was localized not in the plasma membrane but in cytoplasmic organelles or vesicles. These were not related to the photosynthetic membranes as shown by the overlay image. Vesicles marked with BODOPY appeared mainly in peripheral locations in the cell with many of them localizing in the anterior end of the cell, in the place not occupied by the chloroplast and the part of the cytoplasm that seemed to protrude in many algal cells treated with toxic dendrimers (confocal and TEM images, see Figs. 2 and 3).

In order to relate these affected vesicles with mitochondria, two MitoTracker probes were used: MitoTracker Green FMwhich accumulates in the mitochondria and MitoTracker Orange CM-H2 TM ROS which is widely used as indicator of mitochondrial reactive oxygen species. MitoTracker Green FM targets

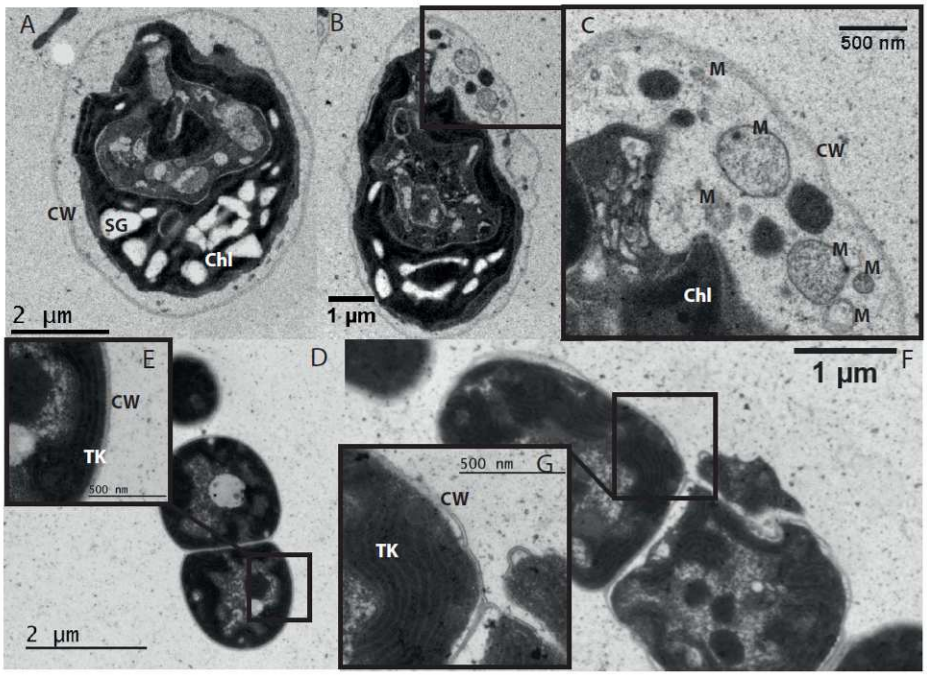

Figure 3. Representative TEM images illustrating the cytoplasmic protrusion observed in *C. reinhardtii* and the envelope disruption in *Anabaena* PCC7120 exposed to -NH_2 PAMAM dendrimers. (A) Control untreated *C. reinhardtii* cell. (B) *C. reinhardtii* cell exposed during 48h to 1.5 mg/L of G2-NH_2 PAMAM dendrimers. (C) Details of *C. reinhardtii* cells exposed to 1.5 mg/L of G2-NH_2 PAMAM dendrimers. (E, D) *Anabaena* PCC7120 untreated control cell. (F, G) details of *Anabaena* PCC7120 exposed during 24h to 1.5 mg/L of -NH_2 PAMAM dendrimers. CW=Cell wall; SG= Starch granule, Chl=Chloroplast; M=Mitochondrion; TK=Thylakoid

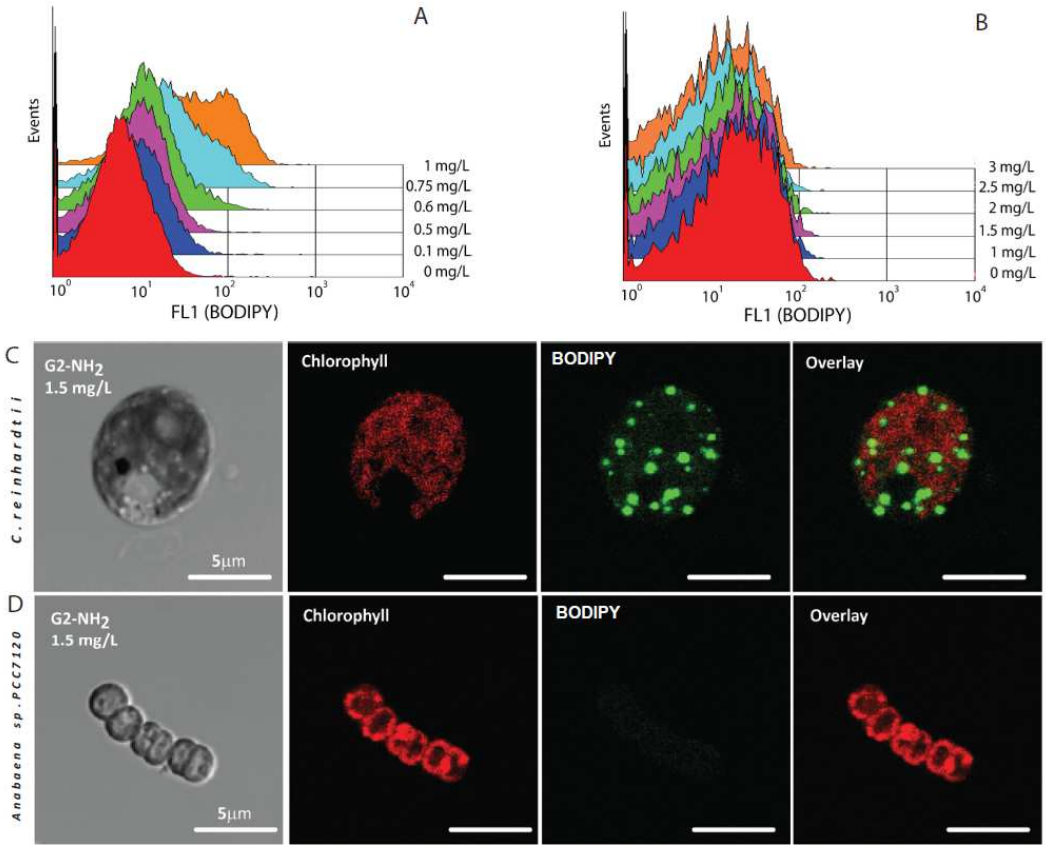

Figure 4. Lipid peroxidation as marked by BODIPY (480/528nm) occurred in *C. reinhardtii* but not in *Anabaena* PCC7120 cells exposed to -NH_2 PAMAM dendrimers. Representative frequency histograms of FL1 channel of (A) *C. reinhardtii* and (B) *Anabaena* PCC7120 exposed to increasing concentrations of G2-NH_2 PAMAM dendrimers during 48h of exposure. Representative confocal images of (C) *C. reinhardtii* and (D) *Anabaena* PCC7120 cells exposed to 1.5 mg/L of G2-NH_2 PAMAM dendrimers showing cellular localization of BODIPY signal. Images are (left to right): bright field, chlorophyll fluorescence (red), BODIPY fluorescence (green) and overlay.

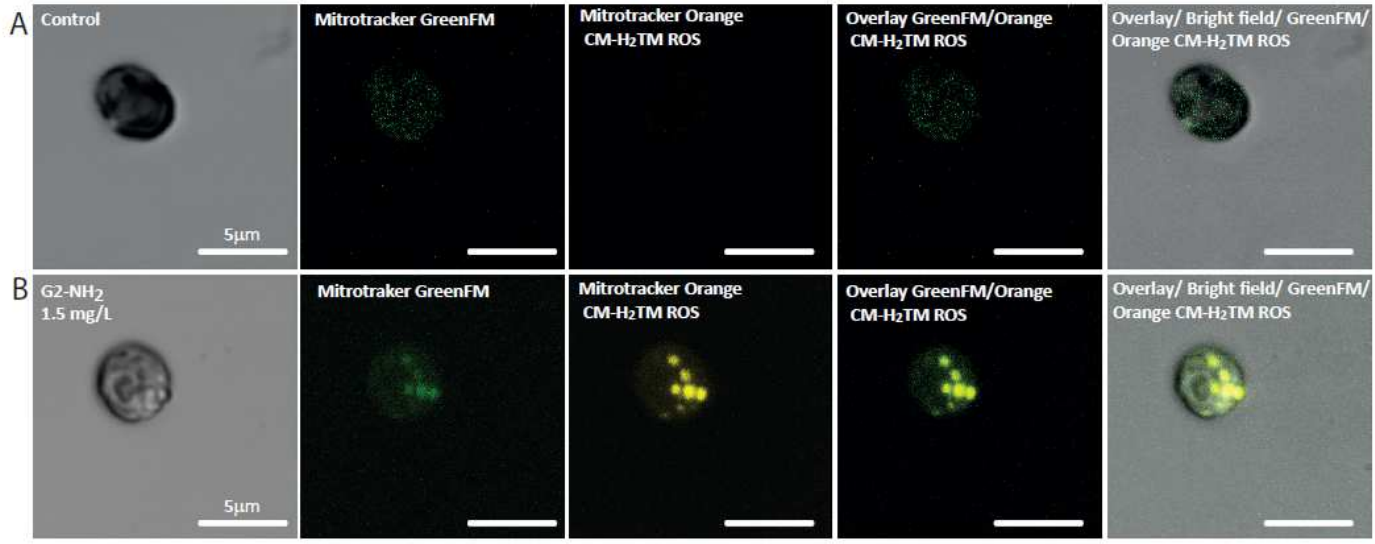

Figure 5. Intracellular localization of mitochondria and mitochondrial oxidation induced by $–NH_2$ PAMAM dendrimers. Representative confocal images of (A) *C. reinhardtii* control cells and (B) *C. reinhardtii* cells exposed during 24h to 1.5 mg/L of G2-NH_2 PAMAM dendrimers. Images are (left to right) bright field, mitochondria (Mitotracker Green FM), mitochondrial oxidation (Mitotracker Orange CM-H2 ROS), overlay of Mitotracker Green FM and Mitotracker Orange CM-H_2 ROS images and overlay of bright field, Mitotracker Green FM and Mitotracker Orange CM-H_2 ROS images.

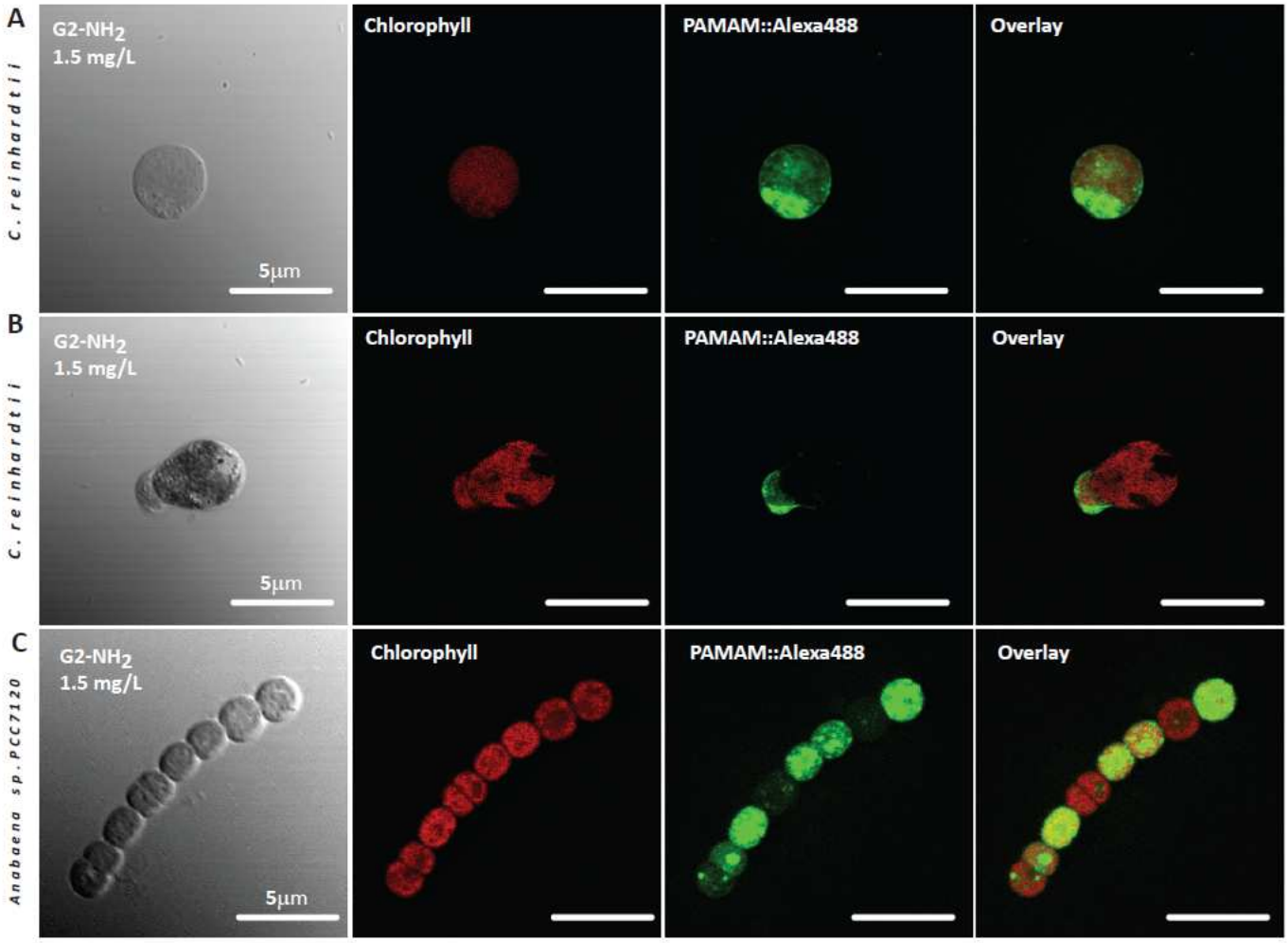

Figure 6. Cellular localization of PAMAM dendrimers conjugated to Alexa Fluor 488 in *C. reinhardtii* (A, B) after 24 h incubation with 1.5 mg/L of G2-NH_2; *Anabaena*PCC7120 cells (C) after24 h incubation with 1.5 mg/L of G2-NH_2. Images are (left to right): bright field, chlorophyll fluorescence (red), DCF fluorescence (green) and overlay.

mitochondria and, as shown in Fig. 5, the green fluorescence was homogenously distributed in non-treated cells (Fig. 5A) while there was a clear condensation in a certain area of the dendrimer-exposed cells (Fig. 5B) which correlated with the locations where mitochondria seemed to condense (Fig. 3). The results with MitoTracker Orange CM-H2 TM ROS, which fluoresces orange when oxidized (Fig 5), and those of BODIPY (Fig. 4) clearly indicated that dendrimer toxicity was related to an increase in ROS formation and lipid peroxidation in mitochondria. In the case of the cyanobacterium (Fig. 4D), no BODIPY fluorescence was recorded, indicating that membrane lipid peroxidation was not involved in the toxic response of this organism: the cyanobacterium is a prokaryotic organism with no intracellular organelles with the exception of the photosynthetic membranes (thylakoids) which did not seem to be functionally affected by dendrimers.

3.4. Internalization of cationic dendrimers

It has been found that dendrimers are internalized in different animal and human cell systems (Albertazzi et al., 2010, Leroueil et al., 2007, Nel et al., 2009, Shukla et al., 2006, Tajarobi et al., 2001). However, to our knowledge, there are no reports in the literature of dendrimer internalization into organisms of environmental relevance such as algae and cyanobacteria. To study whether PAMAM dendrimers were also internalized in the green alga and the cyanobacterium, we conjugated the cationic dendrimers with Alexa Fluor 488 to yield green-labelled PAMAM dendrimers. The AlexaFluor conjugates can be easily detected by flow cytometry and confocal microscopy. Because cationic dendrimers show a high affinity for negatively charged cell surfaces, in order to distinguish between true cell dendrimer internalization and cell-surface bound dendrimers we used a specific anti Alexa 488 antibody. This antibody is unable to cross cellular membranes and upon binding, it effectively quenches the fluorescence of cell-surface bound Alexa Fluor 488-dendrimer conjugates, so that only conjugates internalized into the cell are visualized. Firstly, we determined the rate of cell uptake in the absence and presence of the antibody (Table S1 and Fig. S5).

The data indicated that in the green alga, the three dendrimers were quickly internalized (71% of G2,74% ofG3 and 100% of G4 after 10 min calculated as described in Table S1). In the cyano bacterium dendrimer uptake was slower with 100% uptake after 2 h, although G4 dendrimer uptake was slightly quicker than that of the other two for the shorter time assayed. The experiments showed that in both organisms the Alexa Fluor-dendrimer conjugates were largely internalized even at the shorter time assayed (10 min) with very low retention times in the cell surfaces. Fig.6 shows confocal micrographs of internalized Alexa-dendrimer conjugates in the green alga (Fig. 6A and B) and in the cyanobacterium (Fig. 6C). In the green alga, most of the fluorescence was located at the anterior end of the cell where the cellular deformities have been observed (more clearly seen in Fig. 6B), the overlay image shows that the Alexa-dendrimer conjugates did not localize in the chloroplast. Taking into account the results with the MitoTracker probes (Fig. 5), it is tempting to suggest that the dendrimers were localizing in the mitochondria which get condensed in cell deformities (TEMimages, Fig. 3C). Fig. 6C shows a representative cyanobacterial filament. It is clear that the dendrimers have been internalized and distributed throughout the cytoplasm. Curiously, cells in division showed less internalization. The overlay images showed that, in general, the dendrimers did not localize in the photosynthetic membranes, which correlates with the lack of ROS formation and the lack of effect of dendrimers on photosynthesis.

4. Discussion

Most studies up to date have found that toxicity of PAMAM dendrimers in different cell systems depends on generation (size), dose, exposure duration, species and nature (charge) of the terminal groups (Jain et al., 2010, Malik et al., 2000, Roberts et al., 1996). These studies have been performed on animal or human cell lines/organisms due to their interest in biomedical-related research and reported that low generation PAMAM dendrimers are not toxic or less toxic than their higher generation counterparts (Jevprasesphant et al., 2003, Malik et al., 2000, Roberts et al., 1996). There are just a few reports in the literature concerning the toxicity of dendrimers on organisms of environmental relevance; in fact this is the first report on cyanobacteria. Regarding algae, Petit et al. (2010) also found an increased toxicity with increasing generation number of cationic dendrimers in *Chlamydomonas reinhardtii*. Their EC_x values were one order of magnitude higher than the ones found in our study, the difference being possibly due to the different toxicity endpoint considered. Petit et al. (2010) used cell viability (measured as esterase activity) and we have used direct measurements of growth inhibition. Most studies found that dendrimers with cationic amine terminal groups (and therefore positively charged) are generally more toxic than hydroxyl-terminated dendrimers (Brazeau et al., 1998, Jevprasesphant et al., 2003, Malik et al., 2000, Chen et al., 2004) This is because cationic dendrimers interact with negatively charged functional groups in cell membranes, destabilizing them and eventually resulting in cell lysis (Hong et al., 2006, Rittner et al., 2002). Our results also show that cationic PAMAM of the G2 and G3 generation dendrimers were more toxic to both the green alga and the cyanobacterium than their hydroxyl-terminated counterparts. The role of surface charge (ζ-potential) was clear as the most toxic cationic dendrimers G3-NH2 and G4-NH2 also had the highest net positive charge in the culture media (Table 1). However, both G4 dendrimers showed similar toxicity, indicating that charge is not the only parameters affecting dendrimer toxicity in both microorganisms.

The amino-terminated cationic dendrimers and G4-OH significantly increased the formation of ROS in the green alga and the cyanobacterium. ROS production correlated with the growth inhibition of both organisms. Optical micrographs revealed that ROS formation was not related with the chloroplast or with photosynthetic membranes, showing diffuse distribution in the cyanobacterium and concentrating in protrusions or deformities in the cytoplasm of the green alga. In fact, photosystem II photochemistry was not damaged. Petit et al. (2012) found that G4-NH2 induced ROS formation in *C. reinhardtii* but their results suggested that photosynthetic processes were affected by the dendrimer.

TEM micrographs of the green alga revealed cell damage due to dendrimer exposure with cell ultrastructure disorganization and clustered mitochondria. Fluorescent probes showed that dendrimer toxicity was related to an increase in ROS formation and lipid peroxidation in these organelles. In the cyanobacterium, cell wall and membrane disruption with apparent loss of cytoplasmic contents was found; although no similar studies have been undertaken with prokaryotic organisms such as cyanobacteria, it is well known that cationic nanoparticles may interact with negatively charged membranes producing nanoholes, membrane thinning and disruption (Nel et al., 2009).

We report for the first time that cationic PAMAM dendrimers (in Alexa-dendrimer conjugates) were quickly and largely internalized by the green alga and the cyanobacterium with very low retention in cell surfaces. Most of the dendrimer-conjugate fluorescence was located in the cellular deformities/protrusions of green algae where damaged mitochondria clustered; in the cyanobacterium, the fluorescence was more diffusely distributed although for both alga and cyanobacterium, the Alexa-dendrimer conjugates did not localize in the chloroplast or photosynthetic membranes. Studies in human cell lines have also shown efficient dendrimer internalization with differences in residence times in the cell membranes probably linked to differences in membrane chemical composition; thus, in addition to molecular size certain factors such as specific modulation of cell membrane by dendrimers might also be involved in their permeability (Albertazzi et al., 2010, Shukla et al., 2006, Tajarobi et al., 2001). In conclusion, it seems that dendrimer uptake and internalization largely depends on the cell type and on specific dendrimer features such as size or charge. In fact, as the generation of cationic PAMAM dendrimers increases, the number of surface NH_2-groups also increase, these surface groups being responsible for the binding to the cell envelopes of both organisms that, as shown by the ζ-potential measurements and the FTIR analyses, possess negatively charged functional groups such as carboxyl moieties which have been found in other cyanobacteria and algae (Dittrich and Sibler, 2005, Hadjoudja et al., 2010, Kiefer et al., 1997). It is not yet clear how PAMAM dendrimers cross the plasma membrane. Direct penetration and endocytosis have been suggested as possible mechanisms of dendrimer entry into the cell (Albertazzi et al., 2010, Leroueil et al., 2007). The mechanisms of dendrimer, and in general, nanoparticle internalization in algae and cyanobacterium are presently unknown. Direct penetration of dendrimers in the cyanobacterium is more plausible since endocytic mechanisms are a fundamental eukaryotic- specific process of membrane trafficking. However, endocytosis like protein uptake has been reported in a bacterium (Lonhienne et al., 2010) and more recently, it has been suggested that cyanobacteria use classical endocytosis and macropynocytosis to internalize exogenous GFP (Liu et al., 2013). In the case of the green alga, a eukaryotic organism, very little is known about endocytosis although clathrin-coated vesicles have been purified from this alga (Denning and Fulton, 1989). The intracellular fate is also not clear because very little is known about the endosomal system of green algae. Our data suggest that in the alga internalized dendrimers target mitochondria, resulting in oxidative stress in these organelles which are essential for the bioenergetics of the organism as well as in apoptotic processes. Independently of the internalization mechanisms, the fact that cationic PAMAM dendrimers are quickly and efficiently internalized by organisms of high ecological relevance in aquatic ecosystems such as green algae and cyanobacteria may pose a serious environmental issue due to the observed cytotoxicity.

5. Conclusions

The toxicity of macromolecules designed for medical applications has been rarely assessed for environmental microorganisms such as algae and cyanobacteria which are at the base of food webs and are determinant for the health of ecosystems. We showed that both types of organisms were very sensitive to dendrimers particularly cationic ones although a generation effect was also patent as the hydroxyl-terminated G4-OH was very toxic to both. We showed that damage proceeded due to the production of reactive oxygen species and cell ultra-structural disorganization, although remarkably photosynthesis seemed unaffected; cationic dendrimers were largely and quickly internalized in both types of organisms showing a diffuse distribution in cyanobacteria and affecting mitochondria in algal cells. These results confirm the potential danger of the eventual release of PAMAM dendrimers to the environment and provide relevant data towards effective risk assessment of this kind of nanomaterials.

Acknowledgements

The Spanish MINECO CTM2013-45775-C2-1-R, CTM2013-45775-C2-2-R and CTM2008-04239/TECNO grants supported this study. The authors wish to thank the Flow Cytometry, FTIR and Confocal Microscopy services from the SIDI-UAM for their excellent technical assistance.

References

ALBERTAZZI, L., SERRESI, M., ALBANESE, A. & BELTRAM, F. 2010. Dendrimer internalization and

intracellular trafficking in living cells. Mol Pharm, 7, 680-8.
BRAZEAU, G. A., ATTIA, S., POXON, S. & HUGHES, J. A. 1998. In vitro myotoxicity of selected cationic macromolecules used in non-viral gene delivery. Pharm Res, 15, 680-4.
CAMINADE, A. M., LAURENT, R. & MAJORAL, J. P. 2005. Characterization of dendrimers. Adv Drug Deliv Rev, 57, 2130-46.
CHEN, H.-T., NEERMAN, M. F., PARRISH, A. R. & SIMANEK, E. E. 2004. Cytotoxicity, Hemolysis, and Acute in Vivo Toxicity of Dendrimers Based on Melamine, Candidate Vehicles for Drug Delivery. Journal of the American Chemical Society, 126, 10044-10048.
CHU, B. 2008. Dynamic light scattering. In: BORSALI, R. & PECORA, R. (eds.) Soft Matter Characterization. Berlin, Germany: Springer-Verlag.
DENNING, G. M. & FULTON, A. B. 1989. Purification and characterization of clathrin-coated vesicles from Chlamydomonas. J Protozool, 36, 334-40.
DITTRICH, M. & SIBLER, S. 2005. Cell surface groups of two picocyanobacteria strains studied by zeta potential investigations, potentiometric titration, and infrared spectroscopy. Journal of Colloid and Interface Science, 286, 487-495.
GEOFFROY, L., GILBIN, R., SIMON, O., FLORIANI, M., ADAM, C., PRADINES, C., COURNAC, L. & GARNIER-LAPLACE, J. 2007. Effect of selenate on growth and photosynthesis of *Chlamydomonas reinhardtii*. Aquat Toxicol, 83, 149-58.
GOMES, A., FERNANDES, E. & LIMA, J. L. 2005. Fluorescence probes used for detection of reactive oxygen species. J Biochem Biophys Methods, 65, 45-80.
GOODENOUGH, U. W. & HEUSER, J. E. 1985. The Chlamydomonas cell wall and its constituent glycoproteins analyzed by the quick-freeze, deep-etch technique. J Cell Biol, 101, 1550-68.
HADJOUDJA, S., DELUCHAT, V. & BAUDU, M. 2010. Cell surface characterisation of *Microcystis aeruginosa* and *Chlorella vulgaris*. Journal of Colloid and Interface Science, 342, 293-299.
HEIDEN, T. C., DENGLER, E., KAO, W. J., HEIDEMAN, W. & PETERSON, R. E. 2007. Developmental toxicity of low generation PAMAM dendrimers in zebrafish. Toxicol Appl Pharmacol, 225, 70-9.
HONG, S., LEROUEIL, P. R., JANUS, E. K., PETERS, J. L., KOBER, M. M., ISLAM, M. T., ORR, B. G., BAKER, J. R., JR. & BANASZAK HOLL, M. M. 2006. Interaction of polycationic polymers with supported lipid bilayers and cells: nanoscale hole formation and enhanced membrane permeability. Bioconjug Chem, 17, 728-34.
JAIN, K., KESHARWANI, P., GUPTA, U. & JAIN, N. K. 2010. Dendrimer toxicity: Let's meet the challenge. Int J Pharm, 394, 122-42.
JEVPRASESPHANT, R., PENNY, J., JALAL, R., ATTWOOD, D., MCKEOWN, N. B. & D'EMANUELE, A. 2003. The influence of surface modification on the cytotoxicity of PAMAM dendrimers. Int J Pharm, 252, 263-6.
KIEFER, E., SIGG, L. & SCHOSSELER, P. 1997. Chemical and Spectroscopic Characterization of Algae Surfaces. Environmental Science & Technology, 31, 759-764.
KIM, S. H. & LAMM, M. H. 2012. Multiscale Modeling for Host-Guest Chemistry of Dendrimers in Solution. Polymers, 4, 463-485.
LEGANES, F., BLANCO-RIVERO, A., FERNANDEZ-PINAS, F., REDONDO, M., FERNANDEZ-VALIENTE, E., FAN, Q., LECHNO-YOSSEF, S. & WOLK, C. P. 2005. Wide variation in the cyanobacterial complement of presumptive penicillin-binding proteins. Arch Microbiol, 184, 234-48.
LEROUEIL, P. R., HONG, S., MECKE, A., BAKER, J. R., JR., ORR, B. G. & BANASZAK HOLL, M. M. 2007. Nanoparticle interaction with biological membranes: does nanotechnology present a Janus face? Acc Chem Res, 40, 335-42.
LIU, B. R., HUANG, Y. W. & LEE, H. J. 2013. Mechanistic studies of intracellular delivery of proteins by cell-penetrating peptides in cyanobacteria. BMC Microbiol, 13, 57.
LONHIENNE, T. G., SAGULENKO, E., WEBB, R. I., LEE, K. C., FRANKE, J., DEVOS, D. P., NOUWENS, A., CARROLL, B. J. & FUERST, J. A. 2010. Endocytosis-like protein uptake in the bacterium *Gemmata obscuriglobus*. Proc Natl Acad Sci U S A, 107, 12883-8.
MALIK, N., WIWATTANAPATAPEE, R., KLOPSCH, R., LORENZ, K., FREY, H., WEENER, J. W., MEIJER, E. W., PAULUS, W. & DUNCAN, R. 2000. Dendrimers: relationship between structure and biocompatibility in vitro, and preliminary studies on the biodistribution of 125I-labelled polyamidoamine dendrimers in vivo. J Control Release, 65, 133-48.
MARKER, A. F. H. 1972. The use of acetone and methanol in the estimation of chlorophyll in the presence of phaeophytin. Freshwater Biology, 2, 361-385.
MAXWELL, K. & JOHNSON, G. N. 2000. Chlorophyll fluorescence--a practical guide. J Exp Bot, 51, 659-68.
MENJOGE, A. R., KANNAN, R. M. & TOMALIA, D. A. 2010. Dendrimer-based drug and imaging conjugates: design considerations for nanomedical applications. Drug Discov Today, 15, 171-85.
MORTIMER, M., KASEMETS, K., HEINLAAN, M., KURVET, I. & KAHRU, A. 2008. High throughput kinetic *Vibrio fischeri* bioluminescence inhibition assay for study of toxic effects of nanoparticles. Toxicol In Vitro, 22, 1412-7.
MUKHERJEE, S. P., DAVOREN, M. & BYRNE, H. J. 2010. In vitro mammalian cytotoxicological study of PAMAM dendrimers - towards quantitative structure activity relationships. Toxicol In Vitro, 24, 169-77.
NAHA, P. C., DAVOREN, M., CASEY, A. & BYRNE, H. J. 2009. An ecotoxicological study of poly(amidoamine) dendrimers-toward quantitative structure activity relationships. Environ Sci Technol, 43, 6864-9.
NEL, A. E., MADLER, L., VELEGOL, D., XIA, T., HOEK, E. M., SOMASUNDARAN, P., KLAESSIG, F., CASTRANOVA, V. & THOMPSON, M. 2009. Understanding biophysicochemical interactions at the nano-bio interface. Nat Mater, 8, 543-57.
PERREAULT, F., BOGDAN, N., MORIN, M., CLAVERIE, J. & POPOVIC, R. 2012. Interaction of gold nanoglycodendrimers with algal cells (*Chlamydomonas reinhardtii*) and their effect on physiological processes. Nanotoxicology, 6, 109-20.
PETIT, A. N., DEBENEST, T., EULLAFFROY, P. & GAGNE, F. 2012. Effects of a cationic PAMAM dendrimer on photosynthesis and ROS production of

Chlamydomonas reinhardtii. Nanotoxicology, 6, 315-26.

PETIT, A. N., EULLAFFROY, P., DEBENEST, T. & GAGNE, F. 2010. Toxicity of PAMAM dendrimers to *Chlamydomonas reinhardtii*. Aquat Toxicol, 100, 187-93.

PORRA, R. J., THOMPSON, W. A. & KRIEDEMANN, P. E. 1989. Determination of accurate extinction coefficients and simultaneous equations for assaying chlorophylls a and b extracted with four different solvents: verification of the concentration of chlorophyll standards by atomic absorption spectroscopy. Biochimica et Biophysica Acta (BBA) - Bioenergetics, 975, 384-394.

RITTNER, K., BENAVENTE, A., BOMPARD-SORLET, A., HEITZ, F., DIVITA, G., BRASSEUR, R. & JACOBS, E. 2002. New basic membrane-destabilizing peptides for plasmid-based gene delivery in vitro and in vivo. Mol Ther, 5, 104-14.

ROBERTS, J. C., BHALGAT, M. K. & ZERA, R. T. 1996. Preliminary biological evaluation of polyamidoamine (PAMAM) Starburst dendrimers. J Biomed Mater Res, 30, 53-65.

RODEA-PALOMARES, I., BOLTES, K., FERNÁNDEZ-PINAS, F., LEGANÉS, F., GARCÍA-CALVO, E., SANTIAGO, J. & ROSAL, R. 2011. Physicochemical characterization and ecotoxicological assessment of CeO_2 nanoparticles using two aquatic microorganisms. Toxicol Sci, 119, 135-45.

RODEA-PALOMARES, I., GONZALO, S., SANTIAGO-MORALES, J., LEGANÉS, F., GARCÍA-CALVO, E., ROSAL, R. & FERNÁNDEZ-PINAS, F. 2012. An insight into the mechanisms of nanoceria toxicity in aquatic photosynthetic organisms. Aquat Toxicol, 122-123, 133-43.

SANTIAGO-MORALES, J., ROSAL, R., HERNANDO, M. D., ULASZEWSKA, M. M., GARCÍA-CALVO, E. & FERNÁNDEZ-ALBA, A. R. 2013. Fate and transformation products of amine-terminated PAMAM dendrimers under ozonation and irradiation. J Hazard Mater, 266C, 102-113.

SAOVAPAKHIRAN, A., D'EMANUELE, A., ATTWOOD, D. & PENNY, J. 2009. Surface modification of PAMAM dendrimers modulates the mechanism of cellular internalization. Bioconjug Chem, 20, 693-701.

SHUKLA, R., THOMAS, T. P., PETERS, J. L., DESAI, A. M., KUKOWSKA-LATALLO, J., PATRI, A. K., KOTLYAR, A. & BAKER, J. R., JR. 2006. HER2 specific tumor targeting with dendrimer conjugated anti-HER2 mAb. Bioconjug Chem, 17, 1109-15.

STASKO, N. A., JOHNSON, C. B., SCHOENFISCH, M. H., JOHNSON, T. A. & HOLMUHAMEDOV, E. L. 2007. Cytotoxicity of polypropylenimine dendrimer conjugates on cultured endothelial cells. Biomacromolecules, 8, 3853-9.

SUAREZ, I. J., ROSAL, R., RODRIGUEZ, A., UCLES, A., FERNANDEZ-ALBA, A. R., HERNANDO, M. D. & GARCÍA-CALVO, E. 2011. Chemical and ecotoxicological assessment of poly(amidoamine) dendrimers in the aquatic environment. TrAC Trends in Analytical Chemistry, 30, 492-506.

SUEOKA, N. 1960. Mitotic replication of deoxyribonucleic acid in *Chlamydomonas Reinhardi*. Proceedings of the National Academy of Sciences, 46, 83-91.

SVENSON, S. & TOMALIA, D. A. 2005. Dendrimers in biomedical applications--reflections on the field. Adv Drug Deliv Rev, 57, 2106-29.

TAJAROBI, F., EL-SAYED, M., REGE, B. D., POLLI, J. E. & GHANDEHARI, H. 2001. Transport of poly amidoamine dendrimers across Madin-Darby canine kidney cells. Int J Pharm, 215, 263-7.

UCLÉS, A., ULASZEWSKA, M. M., HERNANDO, M. D., RAMOS, M. J., HERRERA, S., GARCÍA, E. & FERNÁNDEZ-ALBA, A. R. 2013. Qualitative and quantitative analysis of poly(amidoamine) dendrimers in an aqueous matrix by liquid chromatography–electrospray ionization-hybrid quadrupole/time-of-flight mass spectrometry (LC-ESI-QTOF-MS). Analytical and Bioanalytical Chemistry, 405, 5901-5914.

ULASZEWSKA, M. M., HERNANDO, M. D., UCLÉS, A., ROSAL, R., RODRÍGUEZ, A., GARCÍA-CALVO, E. & FERNÁNDEZ-ALBA, A. R. 2012. Chemical and ecotoxicological assessment of dendrimers in the aquatic environment. In: FARRÉ, M. &BARCELÓ, D. (eds.) Analysis and Risk of Nanomaterials in Environmental and Food Samples. Amsterdam: Elsevier.

VAN DER MEI, H. C., NOORDMANS, J. & BUSSCHER, H. J. 1989. Molecular surface characterization of oral streptococci by Fourier transform infrared spectroscopy. Biochim Biophys Acta, 991, 395-8.

XIA, T., KOVOCHICH, M., BRANT, J., HOTZE, M., SEMPF, J., OBERLEY, T., SIOUTAS, C., YEH, J. I., WIESNER, M. R. & NEL, A. E. 2006. Comparison of the abilities of ambient and manufactured nanoparticles to induce cellular toxicity according to an oxidative stress paradigm. Nano Lett, 6, 1794-807.

Supplementary Material

First evidences of PAMAM dendrimer internalization in microorganisms of environmental relevance: A linkage with toxicity and oxidative stress

Soledad Gonzalo‡, Ismael Rodea-Palomares†, Francisco Leganés†, Eloy García-Calvo§, Roberto Rosal‡§, Francisca Fernández-Piñas†*

† Departamento de Biología, Facultad de Ciencias, Universidad Autónoma de Madrid, E-28049, Madrid, Spain

‡ Departamento de Ingeniería Química, Universidad de Alcalá, E-28871, Alcalá de Henares, Madrid, Spain

§ Advanced Study Institute of Madrid, IMDEA-Agua, Parque Científico Tecnológico, E-28805, Alcalá de Henares, Madrid, Spain

* Corresponding author: francisca.pina@uam.es

Contents:

Table S1. Uptake and internalization of Alexa Fluor 488-dendrimer conjugates in *C. reinhardtii* and *Anabaena sp.* PCC 7120 cells.

C. reinhardtii											
	10 min			60 min			240 min			Exponential fit[4]	
	% Uptake[1]	% Surface[2]	% Internalized[3]	% Uptake[1]	% Surface[2]	% Internalized[3]	% Uptake[1]	% Surface[2]	% Internalized[3]	Slope	R^2
G2	71.30	4.30	95.70	72.81	8.76	91.24	100.00	2.20	97.80	0.13	0.98
G3	74.29	6.50	93.50	108.10	1.05	98.95	100.00	-0.40	100.40	0.20	0.97
G4	95.08	3.45	96.55	102.00	9.00	91.00	100.00	2.40	97.60	2.14	0.95
A. PCC 7120											
	% Uptake[1]	% Surface[2]	% Internalized[3]	% Uptake[1]	% Surface[2]	% Internalized[3]	% Uptake[1]	% Surface[2]	% Internalized[3]	Slope	R^2
G2	32.17	7.60	92.40	93.94	-3.50	103.50	100.00	-2.70	102.70	0.04	0.95
G3	30.87	5.40	94.60	85.04	-3.90	103.90	100.00	-1.50	101.50	0.04	0.94
G4	57.45	14.75	85.25	84.26	-2.80	102.80	100.00	-6.20	106.20	0.10	0.96

Cells were exposed to 1.5 mg/L of Alexa 488-dendrimer conjugates G2, G3 and G4, which implied an equivalent exposure in terms of functionalized surface groups (approximately 15 μmol FG/L in all cases). Fluorescence was measured by flow cytometry (488/528 nm).

[1]: % Uptake for each time-point was derived by taking as reference the maximum emission recorded for each treatment along the experimental time course as follows: % Uptake = (Fluor $528t_i$/Fluor $528t_{max}$)*100. Where Fluor $528t_i$ and Fluor $528t_{max}$ were the mean fluorescence signal at 528nm at time t_i and the maximum mean fluorescence at 528nm, respectively.

[2,3]: % Surface and % Internalized were estimated based on the anti-Alexa 488 experiments as follows: % Internalized = ($Fluor_{quenched}$ $528t_i$ / Fluor $528t_i$)*100; % Surface = (100- % Internalized). Where $Fluor_{quenched}$ $528t_i$ and Fluor $528t_i$ were the mean fluorescence signals at 528nm at time t_i with and without anti-Alexa488 treatment, respectively.

[4]: % uptakes were fitted by the following exponential model: y = A*(1 - exp(-k*(x-xc))). Were K is the slope of the exponential rise. R^2 accounts for the goodness of fit. Fitted functions and equation parameters are provided in Supplementary Figure S5

Table S2. Dose-effect parameters of toxicity (as growth inhibition) induced by PAMAM dendrimers for both *Chlamydomonas reinhardtii* and *Anabaena* sp. PCC7120 after 72 h of exposure.

Chlamydomonas reinhardtii						
Compound	Model fitted[1]	Max. Stimulation[2]	Max. Inhibition[3]	EC_{10} (µM)	EC_{50} (µM)	EC_{90} (µM)
G2-OH	-	-	-30%	-	-	-
G3-OH	-	-	-50%	-	-	-
G4-OH	BC.5	0.018 (50%)	-	0.03^{a}(0.029-0.033)	0.052^{a}(0.049-0.055)	0.071^{a}(0.064-0.079)
G2-NH2	LL2.3u	-	-	0.153^{b}(0.150-0.160)	0.178^{b}(0.175-0.181)	0.218^{b}(0.212-0.227)
G3-NH2	W2.4	-	-	0.063^{c}(0.059-0.067)	0.081^{c}(0.069-0.093)	0.094^{c}(0.075-0.111)
G4-NH2	W1.4	-	-	0.038^{d}(0.037-0.039)	0.047^{d}(0.047-0.049)	0.054^{d}(0.053-0.057)
Anabaena sp. PCC7120						
Compound	Model fitted	Max. Stimulation	Max Inhibition	EC_{10} (µM)	EC_{50} (µM)	EC_{90} (µM)
G2-OH	-	3 (5%)	0%	-	-	-
G3-OH	-	1.44 (5%)	0%	-	-	-
G4-OH	W1.3	-	-	0.187^{a}(0.127-00.248)	0.279^{a}(0.248-0.310)	0.360^{a}(0.316-0.406)
G2-NH2	LN.2	-	-	0.328^{a}(0.221-0.433)	0.540^{b}(0.458-0.623)	0.890^{b}(0.633-1.155)
G3-NH2	LL.3u	-	-	0.312^{a}(0.271-0.356)	0.370^{c}(0.352-0.392)	0.422^{c}(0.381-0.466)
G4-NH2	BC.5	-	-	0.180^{b}(0.163-0.193)	0.230^{d}(0.208-0.248)	0.318^{a}(0.265-0.360)

Statistically significant differences (ANOVA, *post hoc*, $p < 0.05$) for the different effective concentrations (EC_x) are indicated by superscript letters.

[1]: Model fitted: Fitted models were selected based on the best fit offered by drc package for R. Notation for the selected fitted models is according to drc notation: BC.5. Brain cousens model, LL2.3u: Log-logistic 2.3 U shaped, W2.4: Weibull model 2.4, W1.4: Weibull model 1.4, W1.3: Weibull model 1.3, LN.2: Log-normal 2 parameters model, LL.3u: Log-logistic three parameters,

[2]: Max. Stimulation: Concentration at which the maximum stimulation occurred together with the % of stimulation (between parentheses) of the studied end-point respect to the control level.

[3]: Max. Inhibition: Concentration at which the maximum inhibition occurred together with the % of inhibition (between parentheses) achieved at that concentration.

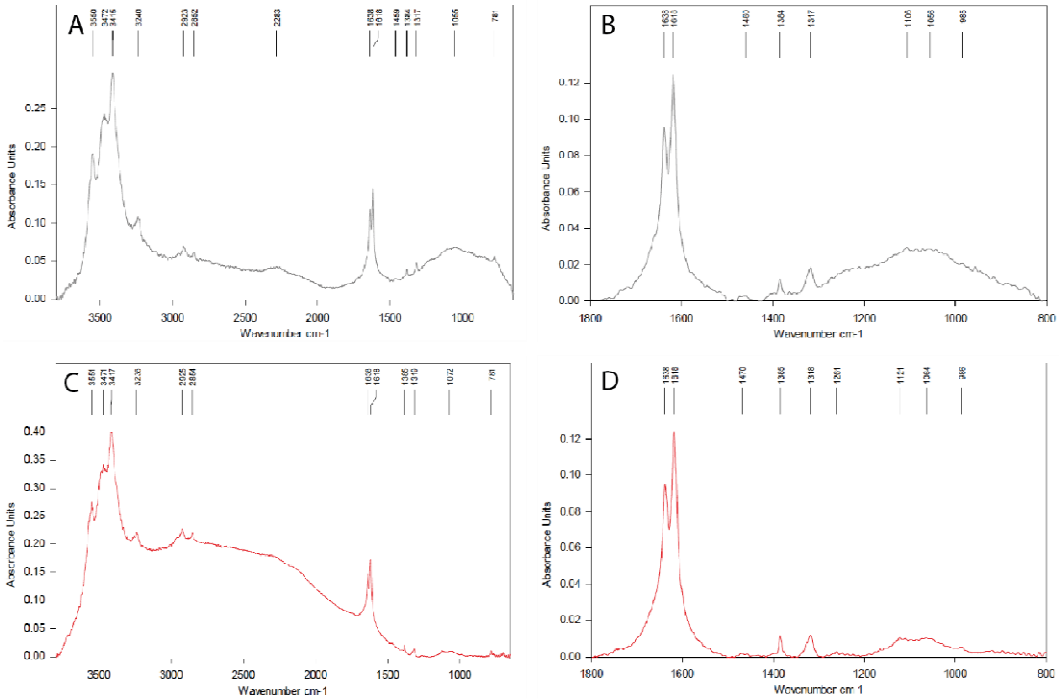

Figure S1. FTIR spectra of *C. reindhartii* (A, B) and *Anabaena sp.* PCC7120 (C,D) cells. FTIR spectra are presented between 4000 cm^{-1} and 800 cm^{-1} (A and C), and more detailed information is given in the fingerprint region (between 1800 cm^{-1} and 800 cm^{-1}; B and D). Main peaks are indicated by arrows. See Table 2 for specific band assignments.

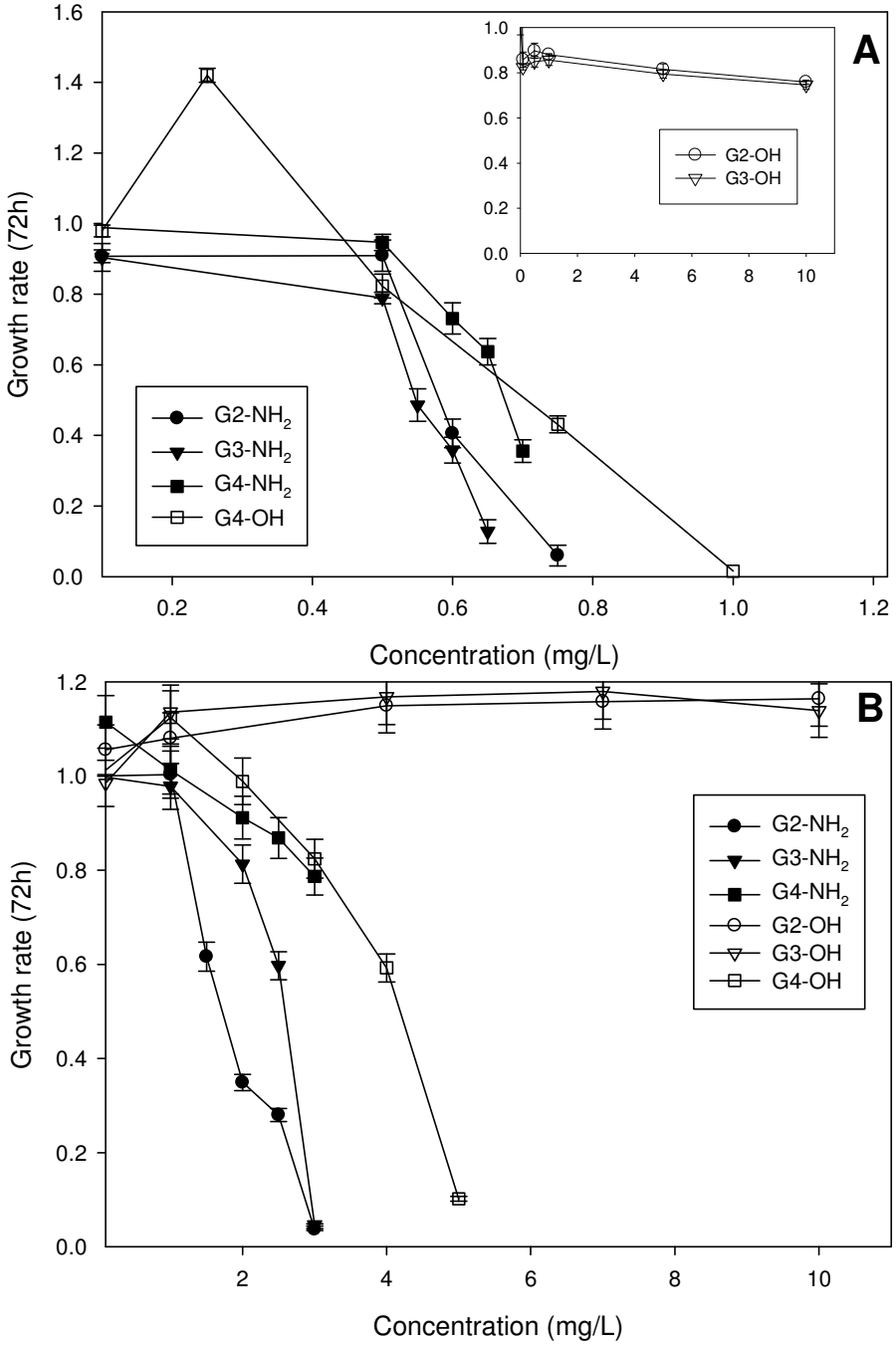

Figure S2. Dose-response curves of *C. reindhartii* (A) and *Anabaena sp.* PCC 7120 (B) exposed to increasing concentrations of $-NH_2$ and –OH G2, G3 and G4 PAMAM dendrimers.

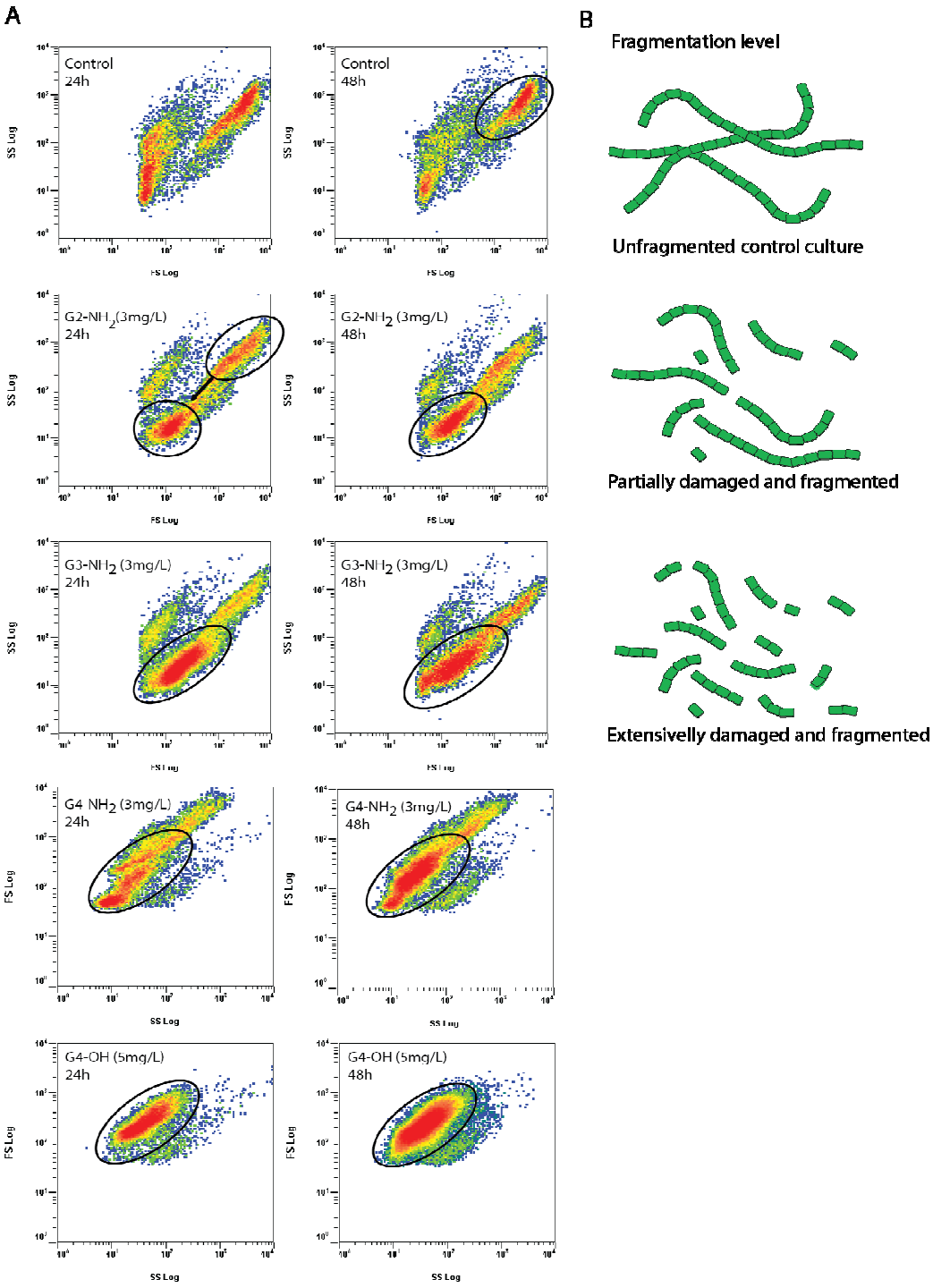

Figure S3. A: FS-SS density plots showing the filament fragmentation of *Anabaena* PCC7120 exposed to G2-NH_2, G3-NH_2, G4-NH_2 and G4-OH PAMAM dendrimers occurring at increasing times of exposure. The color intensity pattern marks increasing densities of events (from blue to red). Circles indicate how the main population size and complexity distribution shifts to less size (FS) and complexity (SS) values with the exposure times in the G2, G3, G4 –NH_2 and G4 –OH treatments. (B) Schematic representation of the different levels of filament fragmentation of *Anabaena* PCC7120 as observed by the microscope.

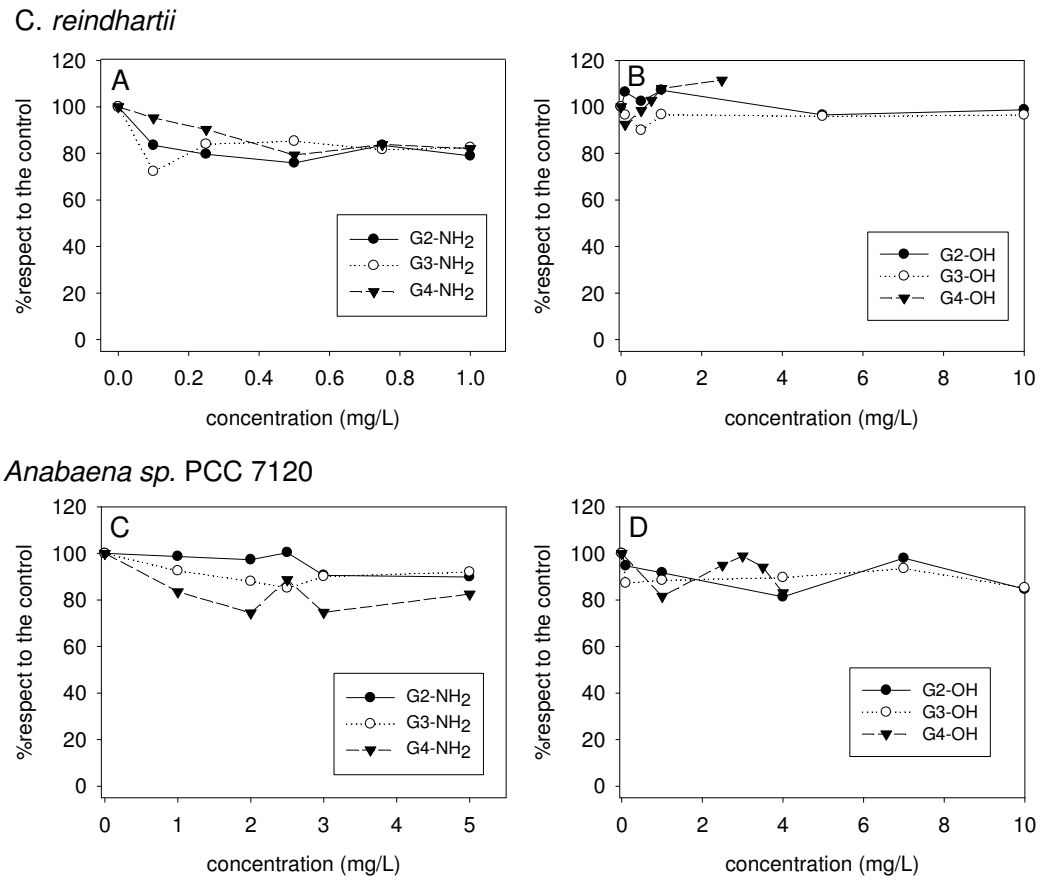

Figure S4. Maximum photosynthetic efficiency (Fv/Fm ratio) of photosystem II (PSII) measured by PAM fluorimetry in *C. Reindartii* cells exposed to increasing concentrations of $–NH_2$ (A) and –OH (B) PAMAM dendrimers, and *A.* PCC 7120 cells exposed to increasing concentrations of $–NH_2$ (C) and –OH (D) PAMAM dendrimers.

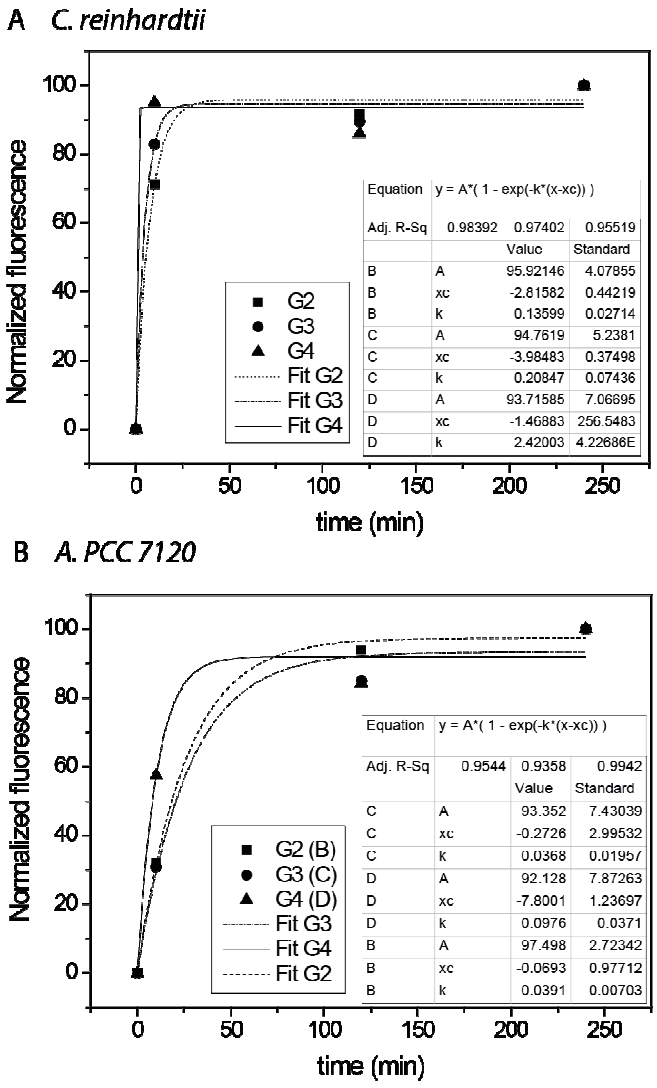

Figure S5. Exponential fit of Alexa Fluor 488-dendrimer conjugates uptake for (A) *C. reinhardtii*, and (B) *Anabaena sp.* PCC 7120.